TURUN YLIOPISTO

Involvement of Singlet Oxygen in Photoinhibition Under Different Light and Temperature Conditions

Master's thesis

University of Turku
Faculty of Science
Department of Biology
Biology Education Track
30 credits

Author:

Otto Rydman

9.6.2025

Turku

Master's thesis

Discipline: Biology
Author: Otto Rydman
Title: Involvement of singlet oxygen in photoinhibition under different light and temperature conditions
Instructors: Docent Esa Tyystjärvi, Docent Kai Ruohomäki
Pages: 58 pages
Date: 9.6.2025

Besides being the source of life and energy in photosynthesis, light can paradoxically cause irreversible damage to photosynthetic machinery. Photoinhibition of photosystem II (PSII) causes light-induced irreversible damage leading to a loss of oxygen evolution and electron transfer activity. Although photoinhibition of PSII has been extensively studied, the exact molecular mechanisms under visible light remain a subject of debate. Singlet oxygen ($^1O_2$) is a reactive oxygen species which is proposed to act as a damaging agent in photoinhibition. In thylakoids, $^1O_2$ is commonly produced via charge recombination reactions in PSII, suggesting a pivotal contribution. This thesis studies the involvement of $^1O_2$ in photoinhibition both *in vitro* and *in vivo* under varied light and temperature conditions. According to theory, the involvement of $^1O_2$ in photoinhibition enhances while moving towards red light region. Results showed positive temperature dependency for photoinhibition *in vitro* in used light conditions, while no temperature dependency was found *in vivo*. The involvement of $^1O_2$ was assessed using deuterium oxide (D_2O), which prolongs $^1O_2$ lifetime, and a *Synechocystis* sp. PCC 6803 ΔsigCDE strain, presumed to be resistant to $^1O_2$ due to its high carotenoid content. Photoinhibition progressed more slowly in D_2O than in water-surroundings, suggesting a minor effect of $^1O_2$ in photoinhibition. At the same time, ΔsigCDE showed slight resistance in red light compared to the control strain, which could conversely point to a potential role of $^1O_2$ in photoinhibition. Interestingly, deviation from the first-order kinetics in photoinhibition was found both *in vitro* and *in vivo* experiments.

Keywords: photosynthesis, photosynthetic electron transport chain, photoinhibition of photosystem II, singlet oxygen

Pro gradu -tutkielma

Oppiaine: Biologia
Tekijä: Otto Rydman
Otsikko: Singlettihapen osallistuminen fotoinhibitioon eri valo- ja lämpötilaolosuhteissa
Ohjaajat: dosentti Esa Tyystjärvi, dosentti Kai Ruohomäki
Sivumäärä: 58 sivua
Päivämäärä: 9.6.2025

Valon ollessa elämän ja energian edellytys fotosynteesille voi se myös ristiriitaisesti aiheuttaa peruuttamatonta vahinkoa fotosynteesikoneistossa. Fotosysteemi II:n (PSII) fotoinhibitio aiheuttaa irreversiibeliä valovauriota, joka johtaa hapen muodostumiskyvyn ja elektroninsiirtoaktiivisuuden menetykseen. Vaikka PSII:n fotoinhibitiota on tutkittu laajalti jo usean vuosikymmenen ajan, tarkoista molekulaarisista mekanismeista näkyvän valon alueella ei olla edelleenkään yhtä mieltä. Singlettihappi ($^1O_2$) on reaktiivinen happiyhdiste, jonka on ehdotettu toimivan valovaurion aikaansaajana fotoinhibitiossa. Tylakoideissa $^1O_2$:a muodostuu rekombinaatioreaktioiden seurauksena PSII:ssa, mikä tekee siitä otollisen valovaurion aiheuttajan PSII:n fotoinhibitiossa. Tässä tutkielmassa havainnollistan $^1O_2$:n osallisuutta fotoinhibitiossa *in vitro* - ja *in vivo* -kokeilla muuttamalla valo- ja lämpötilaolosuhteita. Teorian mukaan $^1O_2$:n osallisuus fotoinhibitiossa kasvaa liikuttaessa kohti punaisen valon aluetta. Fotoinhibition lämpötilariippuvuus havaittiin olevan positiivista *in vitro* -kokeissa käytetyissä valo-olosuhteissa. Lämpötilariippuvuutta *in vivo* -kokeissa ei löydetty. Tutkielmassani $^1O_2$:n osallisuutta fotoinhibitiossa havainnollistettiin käyttämällä deuteriumoksidia (D_2O) pidentämään $^1O_2$:n elinikää. Lisäksi *Synechocystis* sp. PCC 6803 ΔsigCDE mutanttikantaa käytettiin $^1O_2$:n havainnollistamiseen sen solunsisäisen korkean karotenoidi pitoisuuden vuoksi. Fotoinhibitio D_2O:ssa eteni hitaammin verrattuna vesipohjaiseen liuottimeen, ehdottaen että $^1O_2$:n määrällä liuottimessa on vain vähän vaikutusta fotoinhibitioon. ΔsigCDE kanta osoitti puolestaan punaisessa valossa lievää vastustuskykyä fotoinhibitiolle verrattuna kontrollikantaan, mikä päinvastaisesti ehdottaa $^1O_2$:n mahdollista osallistumista fotoinhibitioon. Lisäksi fotoinhibition havaittiin yllättäen poikkeavan ensimmäisen kertaluvun kinetiikasta molemmissa *in vitro* - ja *in vivo* -kokeissa.

Avainsanat: yhteyttäminen, fotosynteesin elektroninsiirtoketju, fotosysteemi II:n fotoinhibitio, singlettihappi

Table of Contents

1 Introduction

Photosynthesis is one of the most important processes that enables life on Earth. It is a crucial process, where light energy is utilized to produce energy in its biological form for all living organisms to use. Among the living organisms, plants, algae and some bacteria are capable of oxygenic or anoxygenic photosynthesis. In addition, from the evolutionary point of view, oxygenic photosynthesis has also enabled the oxygen dependent life on Earth. Some 3.7–2.7 billion years ago, the ancestor of common cyanobacteria evolved the ability to extract electrons from water enabling the formation of molecular oxygen (O_2) (Fischer et al., 2016; Cardona et al., 2019). This led to the Great Oxidation Event approximately 2.45 billion years ago, followed by the formation of the ozone layer (Sessions et al., 2009; Fischer et al., 2016). The accepted endosymbiosis theory explains the universality of photosynthesis (Martin & Kowallik, 1999; Keeling, 2004), with evidence showing that chloroplasts of plants and algae evolved from cyanobacteria. According to the theory, once a free-living cyanobacterium got engulfed into an early form of eukaryotic cell and developed into an organelle, the chloroplast was formed.

Photosynthesis can be roughly divided to two different processes – the light reactions and the dark reactions. In the overall equation of the light reactions, light energy is being used to reduce $NADP^+$ to NADPH and to produce ATP through photophosphorylation. O_2 is being formed from water as a byproduct in oxygenic photosynthesis. In other words, photosynthetic organisms utilize light reactions to capture light energy and convert it to a chemical form, into biological energy. Light reactions take place at the thylakoid membranes, which are located either in the chloroplasts of eukaryotes, or in the cytosol of prokaryotes.

NADPH and ATP formed in light reactions are utilized in dark reactions, where carbon dioxide (CO_2) is assimilated to carbon skeletons to form sugars or carbohydrates. As the name indicates, dark reactions are independent of light or light dependent reactions, as the trapped form of light energy is utilized in the forms of NADPH and ATP. That is to say, energy transformed into biological form in the light reactions once again goes through a metamorphosis, where energy is converted into chemical bonds of carbohydrates that can act further as cells' energy source, or provide several crucial functions in order to cells to survive. The dark reactions use inorganic carbon to create carbohydrates, which enables photosynthetic organisms to act as crucial primary producers for life on Earth. Despite the name, the dark reactions don't take place solely in the dark. In fact, some of the enzymes involved require light in order to remain active (Berry et al., 2013). Dark reactions can also be referred as carbon fixation, C_3 cycle, reductive pentose

phosphate pathway, or, by its founders, the Calvin-Benson-Bassham cycle. In cyanobacteria, the dark reactions take place in the cytosol, whereas in eukaryotes dark reactions take place in stroma of chloroplasts.

1.1 Photosynthetic electron transport chain

Thylakoid membranes hold the apparatus that converts light energy into a chemical form. This apparatus consists of membrane-bound protein complexes and water- or lipid-soluble electron carriers. Together they form the photosynthetic electron transport chain (PETC), where harvested light energy is used to extract electrons and protons from water molecules, in order to evolve NADPH and ATP. At the same time O_2 is also produced. This chain of reactions is mediated by two distinct reaction centers, photosystem II (PSII) and photosystem I (PSI), in where the photochemical reactions occur enabling the photosynthetic electron flow. The electron transport chain connects the two distinct reaction centers in sequence, handling the electron transfer between the centers and making PETC a highly structured and regulated entity. Photosynthetic electron transport, where the main products are NADPH, ATP and O_2, is also referred to as the linear electron transport chain. The other possible photosynthetic electron transport pathway is cyclic electron transport, which occurs around PSI and plastoquinone pool, or around PSI and the cytochrome b_6f complex (Cytb_6f) (Allen, 2003). Cyclic electron transport chain results in production of ATP but not NADPH.

In linear electron transport, electrons extracted from water are being used to reduce $NADP^+$. The reaction series starts from PSII in where water is being oxidized at the oxygen evolving complex (OEC) with the help of light energy. First, in plant cells light energy in the form of photons is harvested by light harvesting complexes (LHCs), which are located near both reaction centers. LHCs can be divided to outer and inner LHCs, based on their location around the reaction center. Chlorophylls in LHCs absorb the light energy and transfer it towards the core of PSII. In cyanobacteria, phycobilisomes form the outer antenna structure around the PSII complexes. Phycobilisomes consist of different kinds of bilin pigments and proteins. Regardless of the organism, structures responsible for harvesting the light energy can be referred to as light-harvesting antenna complexes.

Light energy and the photochemical activity of PSII results charge separation and in formation of a strong oxidant, which is capable of extracting electrons from water molecule. At the same

time, O_2 and protons evolve from split water molecules. This reaction is also called the photolysis of water molecule. In PSII, extracted electrons transport through tyrosine, pigments and plastoquinones to free plastoquinone pool, which is in thylakoid membranes. Electrons are carried through plastoquinone pool to Cytb_6f, from where plastocyanin transfers them to PSI. With the help of harvested light energy by LHCs or phycobilisomes, electrons are transferred from PSI to ferredoxin. PSI acts as a light-driven oxido-reductase, where electrons extracted in the oxidation of plastocyanin are used in the reduction of ferredoxin. In the core of PSI, electrons are transferred trough pigments, phylloquinones and iron-sulfur centers. From ferredoxin electrons are finally transported to ferredoxin $NADP^+$ reductase, which catalyzes the formation of NADPH from $NADP^+$.

The linear electron transport chain is also coupled with proton transportation across the thylakoid membrane from stroma to lumen. Besides the photolysis of water molecule, protons are carried and released into lumen by plastoquinone pool that mediates electron flow between the PSII and Cytb_6f complexes. The proton gradient is later discharged trough the ATP synthase that uses it to catalyze formation of ATP, the other main product of the light reactions.

1.2 Photosystem II

Photosystem II (PSII) acts as a light-driven water-plastoquinone oxidoreductase. That is to say, PSII oxidizes water molecules and reduces plastoquinone with the electrons extracted from water. This photochemical process is made possible with the help of light energy. Structurally the PSII reaction center consists of numerous protein subunits and cofactors that are all embedded in the thylakoid membrane (see for example G. Renger & Renger, 2008; Umena et al., 2011; Wei et al., 2016). In the core complex of the PSII monomer lays four intrinsic protein subunits D1, D2, CP43, and CP47. These four subunits are surrounded by twelve membrane spanning protein subunits: PsbE, PsbF, PsbH, PsbI, PsbJ, PsbK, PsbL, PsbM, PsbTc, PsbW, PsbX, and PsbZ. Finally, four extrinsic subunits, PsbO, PsbP, PsbQ, and PsbTn, are bound to the luminal side of PSII. Between plant cells and cyanobacteria, the core structure of PSII is fundamentally similar, the major differences appearing only at the extrinsic domains and light-harvesting antenna systems (Umena et al., 2011; Wei et al., 2016). At the thylakoid membrane PSII complexes typically occur as homodimers. Additionally, within the PSII homodimer lays over two thousand water molecules, most of them are located at the stromal or luminal side of PSII, but also within the thylakoid membrane region (Umena et al., 2011). In the

supramolecular architecture of PSII complexes, LHCs appear as trimers in the near vicinity of PSII, forming the PSII-LHCII super complexes (Wei et al., 2016). In cyanobacteria, phycobilisomes are responsible for the light harvesting. In plant cell PSII-LHCII super complexes appear usually at the stacked grana thylakoids (Andersson & Anderson, 1980).

Together with the protein subunits chlorophylls, β-carotenes, lipids, two plastoquinones, haem and non-haem irons, manganese atoms, calcium atoms or ions, bicarbonate, and several different compounds act as crucial cofactors in the PSII complexes (Umena et al., 2011; Suga et al., 2015; Wei et al., 2016). Regarding the photochemical and electron transport activity of PSII, the most important cofactors are located at the core of the PSII complexes. In the intrinsic core complex of PSII, the D1 and D2 proteins bind chlorophylls (Chl), pheophytins (Pheo) and plastoquinones that are essential to electron transport activity of PSII. Reaction center chlorophyll P_{680} consists of four chlorophyll *a* molecules that are bound to the D1 and D2 proteins. In addition, the D1 protein binds a special tyrosine residue and the loosely bound plastoquinone Q_B, whereas the D2 protein binds the tightly bound plastoquinone Q_A. The special tyrosine residue bound by the D1 protein is referred to as tyrosine Z (TyrZ), and it plays a crucial role in electron transport activity.

At the luminal side of PSII lays the OEC (also called as water oxidizing complex, WOC), which enables the oxidation of water by the P_{680}^+. OEC active center consists of manganese-oxygen-calcium cluster (Mn_4O_5Ca), which is directly bound to its place through coordinate linkage with amino acid residues of D1 and CP43 proteins (Umena et al., 2011). Amino acid residues of the D1 and CP43 proteins serve as ligands to manganese atoms, while maintaining the structure and oxygen evolving activity of the whole OEC (Service et al., 2010; Umena et al., 2011). In addition, PsbO, PsbQ and PsbP contribute the stabilization and optimization of OEC functions (Umena et al., 2011; Wei et al., 2016). Also, Cl^- ions in the near vicinity of OEC are believed to maintain the coordination environment of Mn_4O_5Ca cluster enabling the oxygen evolving activity OEC (Kawakami et al., 2009; Umena et al., 2011).

1.3 Electron transport in photosystem II

In order for a photosynthetic organism to maintain its photosynthetic activity in the overall sequence of reactions, it is of great importance to safely convert light energy into chemical form, given that the electron transport processes in PSII involve highly oxidative intermediates

and radical species. In light harvesting antenna complexes, light energy is being absorbed by protein bound pigment molecules. Light absorbing pigment molecules in antenna complexes are usually chlorophylls and carotenoids. In addition, phycobilins play an important role as light absorbing pigment in most antenna complexes of cyanobacteria. In plants for example, LHCs contains mostly chlorophyll *a*, chlorophyll *b* and carotenoids. Chlorophyll *b* and carotenoids act as auxiliary pigments, transforming their absorbed light energy to chlorophyll *a*, which is responsible for transferring the light energy towards the core of a PSII. In antenna, light energy is transferred towards the reaction center from one pigment to another via the exciton mechanism. This process can also be described using the Förster mechanism. Apart from light energy being transferred towards the reaction center, it can also transform into fluorescence or heat.

In the core of PSII, transferred or directly absorbed light energy excites reaction center chlorophyll P_{680}. In the excitation of P_{680}, the excitation energy is delocalized among the chlorophylls Chl_{D1}, Chl_{D2}, P_{D1} and P_{D2}, and to some extent among the pheophytins (Pheo), $Pheo_{D1}$ and $Pheo_{D2}$, which are also bound to reaction center core proteins (G. Renger & Renger, 2008). Excitation of P_{680} leads to charge separation and the formation of primary radical pair $[P_{680}^{+}Pheo^{-}]$, where light energy is concretely transformed into chemical form. Time constant for the formation of $[P_{680}^{+}Pheo^{-}]$ is 0.6–21 ps (Takahashi et al., 1987; Meyer et al., 1989; Groot et al., 2005; Vasil'ev et al., 1996). At least two different pathways coexist, where either Chl_{D1} or P_{D1} can act as a primary donor (Novoderezhkin et al., 2007; Romero et al., 2010). Out of these two pathways Chl_{D1} dependent one is more prominent at physiological temperatures (Raszewski et al., 2005; G. Renger & Renger, 2008). In Chl_{D1} dependent pathway Chl_{D1}^{+} gets its electrons from P_{D1}, and P_{D1}^{+} gets its electrons from TyrZ.

After the charge separation, primary radical pair $[P_{680}^{+}Pheo^{-}]$ is quickly stabilized with the help of Q_A bound at the stromal side of the D2 protein. $Pheo^{-}$ transfers its electron to plastoquinone forming $[P_{680}^{+}Q_A^{-}]$. From Q_A^{-} electron is donated further to Q_B, another plastoquinone bound at the stromal side of the D1 protein. To leave its site, Q_B^{-} needs a subsequent electron donation from Q_A^{-}. In order for this to happen, subsequent light absorption and charge separation need to take place to form Q_A^{-}. When examining time constants of electron transform rates, formation of Q_A^{-} from $Pheo^{-}$ takes from 200 to 500 ps (Schatz et al., 1987; Vasil'ev et al., 1996). When Q_A is reduced to Q_A^{-}, the reaction center is said to be closed, and it can't accept another electron from an excited $Pheo^{-}$. The reduction of Q_B by Q_A^{-} takes from 0.2 to 3 ms (De Wijn & Van Gorkom, 2001). Comparing time constants between the formation of Q_B^{-} and Q_B^{2-}, the latter

from Q_B^- and Q_A^- is slower, taking 0.6 to 0.8 ms (De Wijn & Van Gorkom, 2001; G. Renger & Renger, 2008). In addition to the double reduction, reduced Q_B takes two protons from the stroma and forms plastoquinol PQH_2. Plastoquinol leaves its site in the D1 protein and enters the thylakoid membrane, where it donates its electrons to Cyt*b*$_6$*f* and protons to lumen. The empty plastoquinone site of the D1 protein is occupied by oxidized Q_B from the plastoquinone pool. Time constant for Q_A^- oxidation, when the site of Q_B is empty, is 2–3 ms (De Wijn & Van Gorkom, 2001).

Water splitting in the PSII complexes consists of three types of reaction sequences. Two of them are the already mentioned light-induced charge separation and reductive plastoquinol formation from plastoquinone, whereas the third one is water splitting through oxidation (for review, see G. Renger & Renger, 2008; T. Renger, 2009). Light-induced charge separation enables the formation of P_{680}^+, which is a strong oxidant capable of removing electrons from water molecule. P_{680}^+ removes electrons from water in order to return to its native state, P_{680}. The water molecule is a stable compound under physiological conditions, where PSII is the only known enzyme complex that can remove electrons from it. This fact underlines the uniqueness of the water splitting process. In the water splitting, P_{680}^+ repairs its electron deficit with the help of TyrZ and OEC. TyrZ is a redox active amino residue, which mediates the electron transfers between P_{680} and OEC. After each charge separation P_{680}^+ extracts an electron from TyrZ. This results in formation of $TyrZ^+$• radical, which extracts its electrons from OEC. The formation of $TyrZ^+$• is also coupled by a proton transfer reaction from a histidine residue nearby, which is typical for the stabilization of thermodynamics in biological redox processes (T. J. Meyer et al., 2007; G. Renger & Renger, 2008). This proton transfer reaction is thought to participate in a larger hydrogen-bonded network that may serve as an exit channel for protons, directing them toward the luminal side of the thylakoid membrane during proton-coupled electron transfer events (Umena et al., 2011).

In the active site of OEC, electrons are extracted to $TyrZ^+$• from Mn ions of Mn_4O_5Ca cluster. At the active site, two water molecules are oxidized and O_2 and H^+ are evolved, in reaction sequence referred as Kok cycle (Kok et al., 1970). During the cycle, two water molecules are oxidized to O_2, while four protons and four electrons are released. Kok cycle operates through S-state transitions, where each state (from S_0 to S_3) represents the redox state of Mn ions. In the most reduced S_0-state, at least three of the Mn ions at the active site are in the form of Mn^{3+}, while one is in the form of Mn^{4+}. S-state transition is induced by absorption of photon, and a subsequent charge separation, which changes the redox state of Mn^{3+} to Mn^{4+} donating its

electrons to $TyrZ^{+}$• (G. Renger & Renger, 2008). At the same time, with each S-state transition, one proton is released into the lumen (Klauss et al., 2012). Total absorption of four photons is required in the S-state transitions ($S_0 \rightarrow S_1 \rightarrow S_2 \rightarrow S_3 \rightarrow S_0$), in order for O_2 to evolve from two water molecules. Transformation from S_3 to S_0 takes place trough transient S_4-state, where electrons donated from the active Mn_4O_5Ca cluster are replaced with four electrons extracted from two water molecules. During the S_4-state transition, O_2 is released.

1.3.1 Charge recombination reactions in photosystem II

Much like all chemical reactions, the electron transfer reactions in PSII are reversible by their nature. This means that the forward movement of electrons along the PETC is coupled with backward moving electron flow, to form an equilibrium between electron transport reactions in PSII. These reversible electron transport reactions are referred to as charge recombination reactions, where electrons could be transferred back to reaction center from reduced pheophytin ($Pheo^{-}$) or plastoquinone (Q_A^{-} or Q_B^{-}/Q_B^{2-}). In most cases, the equilibrium of electron transfer reactions in the PSII is heavily on the side of products, so the reactions are virtually irreversible. For example, forward moving electron transport is stabilized in the formation of $[P_{680}^{+}Q_A^{-}]$ after primary charge separated state of P_{680}^{+} and $Pheo^{-}$, where $Pheo^{-}$ reduces the Q_A. However, the charge recombination between P_{680}^{+} and $Pheo^{-}$ is common to take place multiple times before the secondary electron transport to Q_A. Charge recombination reactions could also take place trough slower recombination reactions between S-state transitions of OEC and plastoquinones ($S_{2/3}Q_A^{-} \rightarrow S_{1/2}Q_A$ or $S_{2/3}Q_B^{-} \rightarrow S_{1/2}Q_B$ recombination pathways). $S_{2/3}Q_A^{-}$ charge recombination reactions involve direct, indirect, or excitonic pathways (Rappaport et al., 2002). In direct pathway, electron is transferred straight from reduced Q_A^{-} to oxidized P_{680}^{+}. In indirect pathways, electrons are transferred through primary acceptor Pheo to P_{680}^{+}. In the excitonic pathway, reaction center gets re-excited. Secondary electron transport in PSII results in the stabilization of charge separated stages, making the charge recombination reactions more unlikely. However, if the OEC is not functioning and fails to reduce P_{680}^{+} (for example during "misses", see chapter 1.5.1), the recombination of $[P_{680}^{+}Q_A^{-}]$ occurs rapidly (Vass & Styring, 1993).

Charge recombination reactions are linked to formation of singlet oxygen ($^1O_2$), a reactive oxygen species (ROS) that can act as a damaging agent against the photosynthetic apparatus (Vass, 2011). On the other hand, it is also suggested that charge recombination pathways could play a protective role against light-induced damage in PSII (Vass & Cser, 2009). Chlorophyll

molecules occur mainly in their singlet-state, where the electrons at the outermost orbital lay with antiparallel spins. As for the triplet-state, outermost electrons lay in two different orbitals with parallel spins. In the reverse electron flow of the charge recombination reactions, spin configuration of the outermost electron could be spontaneously converted, resulting in the formation of $^3P_{680}$. Formation of $^3P_{680}$ is especially linked with the formation of singlet oxygen (Vass, 2011; Tyystjärvi, 2013).

1.4 Singlet oxygen

ROS are oxygen derived compounds that are commonly more reactive towards biomolecules compared to ground state molecular oxygen, O_2. They are normal by-products of aerobic metabolism, which are involved in good and bad regarding the cell's functions. Due to their reactivity, ROS are considered as harmful compounds that can cause several structural changes and damage through oxidative reactions with biomolecules. However, it should also be underlined that ROS can play a crucial role in plants by acting as signaling molecules, especially under stressful conditions. Common ROS involved in aerobic metabolism are $^1O_2$, hydrogen peroxide (H_2O_2), super oxide ($O_2^{\bullet -}$), hydroxyl radical (HO•), different kinds of peroxides, and lipid radicals (Khorobrykh et al., 2020).

$^1O_2$ is ROS that is commonly formed from O_2 via energy absorption, coupled with interaction with a triplet-state donor molecule, resulting in a spin conversion of one of the unpaired electrons in O_2. In its normal ground state, O_2 is in triplet-state ($^3\Sigma^+_gO_2$), where electrons lay at outermost molecular orbitals with parallel spins. Regarding to Pauli's exclusion principle, two electrons can reside on the same orbital only with antiparallel spins. In O_2, the spin conversion of another unpaired electron leads to a formation of two singlet forms, where electrons with antiparallel spins can lay either in two different orbitals ($^1\Sigma^+_gO_2$) or both in the same orbital ($^1\Delta_gO_2$). In physiological conditions and in biological reactions, $^1O_2$ is commonly in its $^1\Delta_gO_2$ form, because the $^1\Sigma^+_gO_2$ form is rapidly converted to $^1\Delta_gO_2$. Additionally, the lifetime of $^1\Sigma^+_gO_2$ in physiological conditions is estimated to be 10^{-11} s (Krinsky, 1977), making it too shortly lived for chemical reactions in general. Here after, $^1\Delta gO_2$ will be referred as $^1O_2$. General reactions involved in the formation of $^1O_2$ are photosensitization and several chemical reactions involving H_2O_2, $O_2^{\bullet -}$, and other reactive oxygen derivates (Khorobrykh et al., 2020).

Reactivity of $^1O_2$ can be explained by the spin conversion. In O_2, two outermost electrons lay in different orbitals with parallel spins, making it a triplet in its ground-state. This restricts the reactivity between the O_2 and biological compounds. In order to react, reactions can occur through spin conversion with the requirement of additional input of energy. On the other hand, for all compounds, it is common to occur in singlet state. In the case of $^1O_2$, already happened spin conversion enables it to react more rapidly than O_2 with its surrounding biological compounds. Common way to react for $^1O_2$ is with electron rich organic molecules, where it acts as an electrophilic agent. In the context of biomolecules, this involves rapid reactions with proteins, unsaturated fatty acids and nucleic acids (Khorobrykh et al., 2020). A common way for $^1O_2$ to react is also through the physical deactivation of its excess energy. Through this deactivation, $^1O_2$ loses its excitation energy via radiative and non-radiative pathways through collisions with other molecules. Here the solvent of $^1O_2$ plays an important part, where a common way for deactivation of $^1O_2$ is through collisions with solvent molecules (Khorobrykh et al., 2020). For example, in physiological conditions, a common way for physical deactivation of $^1O_2$ is collisions with water molecules. Lifetime of $^1O_2$ in physiological conditions is estimated to be only a few μs in water and 20–25 μs in the lipid bodies (Lee & Rodgers, 1983; Mattila et al., 2015). In deuterium oxide (D_2O), the lifetime of $^1O_2$ is around 64 μs (Schweitzer & Schmidt, 2003). In addition, some estimations from the lifetime of $^1O_2$ in biological settings at the scale of nanoseconds have been made (Khorobrykh et al., 2020).

1.4.1 Formation of $^1O_2$ in thylakoids

In the context of photosynthesis, the production of $^1O_2$ occurs mainly through the interactions between ground-sate O_2 and either excited singlet-state (^{1}Chl*) or triplet-state (^{3}Chl) chlorophylls. These photosensitization reactions involve energy transfers and electron spin conversions, finally leading to formation of $^1O_2$. In the physiological conditions, the reaction between ^{1}Chl* and O_2 is negligible, hence the lifetime of ^{1}Chl* is approximately only 10^{-9} s at its longest (Khorobrykh et al., 2020). As for ^{3}Chl, the lifetime of the compound in anaerobic conditions is 10^{-3} s (Krasnovsky, 1994; Khorobrykh et al., 2020), therefore making it the main source in the formation of $^1O_2$. The formation of ^{3}Chl, on the other hand, is linked either with intersystem crossing or recombination reactions in the reaction centers (Khorobrykh et al., 2020). In the intersystem crossing, excited singlet-state chlorophyll transforms into triplet form via spontaneous spin conversion by one of the outermost electrons. Intersystem crossing mainly

occurs in uncoupled and free chlorophylls (Krieger-Liszkay, 2005). It is also suggested that intersystem crossing might be involved in the formation of ^{3}Chl in LHCs, especially when the light is absorbed by loosely bound chlorophylls in the antennae complexes (Khorobrykh et al., 2020).

The main charge recombination reaction leading to formation of $^1O_2$ is via $^3P_{680}$ in the core of PSII. The formation of $^3P_{680}$ is enabled through recombination reactions that involve [$P_{680}^+Pheo^-$] as a starting point or as an intermediate. Firstly, the recombination of long-lived [$P_{680}^+Pheo^-$] is enabled if the forward electron transport to Q_A is lacking or blocked. In this case, PSII reaction centers enable the formation of $^3P_{680}$ (Krieger-Liszkay, 2005). Even though the recombination of [$P_{680}^+Pheo^-$] could occur numbers of times before the subsequent electron transport, and regardless the state of Q_A, the formation of long-lived radical pair is important for the electron spins to precess. The precession of the spins enables the formation of virtual triplet states more often, resulting in the formation of $^3P_{680}$ (Tyystjärvi, 2013). Normally occurring short-lived recombination of [$P_{680}^+Pheo^-$] doesn't affect the spin configurations of the radical pair, where the recombination of the radical pair is too fast for the precession of the spins to occur (Tyystjärvi, 2013). This leads to the formation of a virtual singlet state that doesn't produce $^3P_{680}$ in its recombination. In the fully functional PSII complexes, the formation of long-lived radical pair is prevented by the secondary electron transport.

The other way for formation of [$P_{680}^+Pheo^-$] is through the back flow of electrons after the first stabilized charge separated state (Vass, 2011). In this pathway, the recombination of the pair [$P_{680}^+PheoQ_A^-$] often produces the virtual triplet-state, ^{3}[$P_{680}^+Pheo^-Q_A$], leading in the formation of $^3P_{680}$ (Pospíšil, 2016). The long lifetime of [$P_{680}^+PheoQ_A^-$] removes the spin correlation, and thus the formation of $^3P_{680}$ via the recombination of ^{3}[$P_{680}^+Pheo^-Q_A$] is favorable (Pospíšil, 2016). Recent finding also links the formation of $^1O_2$ through "miss"-associated formation of [$P_{680}^+PheoQ_A^-$] (Mattila et al., 2023). This reaction would also be expected to favor the formation of $^3P_{680}$, given the lack of spin correlation between the reactants. At room temperature, the triplet-state localization is associated between Chl_{D1} and P_{D1} (Diner et al., 2001), locating the production of $^1O_2$ to D1 protein of PSII.

Triplet-state chlorophyll could also be produced in the core of PSI via charge recombination reactions. In the context of PSI, this results in the formation of $^3P_{700}$. Formation of $^3P_{700}$, however, doesn't lead to a significant amount of $^1O_2$ evolution (Khorobrykh et al., 2020). The production of $^1O_2$ has been detected in isolated PSI-LHCI super complexes at a one-tenth rate

compared to PSII-LHCII production (Cazzaniga et al., 2012). Besides the excited chlorophylls, other known sensitizers in formation of $^1O_2$ are hemes, other tetrapyrroles and iron sulfur centers (Mattila et al., 2015).

1.4.2 Damaging reactions of singlet oxygen

Damaging reactions of $^1O_2$ include structural changes that can lead to a chain of events, affecting overall activity or functions inside the cell. In the case of proteins and protein complexes, $^1O_2$ reacts with double bond containing compounds or electron-rich sulfur atoms (Khorobrykh et al., 2020). Damaging reactions of $^1O_2$ can lead to a loss of enzymatic activity. In thylakoids, this is especially the case with PSII complexes, which act as main producers of $^1O_2$ and minor producers of other ROS (Khorobrykh et al., 2020). In the presence of O_2, and with the addition of external $^1O_2$ sensitizer, PSII complexes have been shown to lose their electron transport activity and pigments are bleached (Mishra et al., 1994; Hideg et al., 2007). These indications are also linked to the suggestion that $^1O_2$ acts as a damaging agent in photoinhibition, even though it hasn't been proved directly (Vass, 2012; Tyystjärvi, 2013). In addition, $^1O_2$ has been linked also to the loss and degradation of the D1 protein (Hideg et al., 2007), affecting the functions of the overall PSII repair cycle (Nishiyama et al., 2004).

As for membrane lipid structures, unsaturated fatty acids are prone to react with $^1O_2$. This reaction leads to the peroxidation of fatty acids, which in turn leads to the formation of other reactive compounds, causing fragmentation of the membrane structure (Khorobrykh et al., 2020). With nucleic acids, $^1O_2$-caused damage targets nucleobases and the sugar moieties of nucleic acids (Di Mascio et al., 2019).

In addition to the damaging reactions of $^1O_2$, it should be underlined that $^1O_2$ could also act as a signaling molecule. These functions make it crucial, especially under stress-induced conditions where $^1O_2$-dependent signaling gives organisms a rapid way to acclimate to the changing conditions. However, the signaling pathways of $^1O_2$ are not fully understood. Due to its reactivity and short lifetime, the diffusion distance of the $^1O_2$ is short to act as a signaling molecule, suggesting that other molecules act as an actual messenger molecule induced by the reaction with $^1O_2$ (Khorobrykh et al., 2020).

1.4.3 Protective mechanisms against singlet oxygen

Several compounds act in the detoxification of $^1O_2$ via different quenching and scavenging mechanisms. In quenching, the excess energy of $^1O_2$ is dissipated via physical deactivation. Besides the direct physical quenching of $^1O_2$, the blocking of the formation of ^{3}Chl could be considered a protective mechanism against $^1O_2$. This involves non-photochemical quenching (NPQ), which plays an important role in the protection from excess light energy (see section 1.5.5). In chemical scavenging reactions, $^1O_2$ is transformed into less harmful compounds via non-enzymatic pathways. Scavenging of $^1O_2$, is done through the non-enzymatic pathways with the interactions of different kinds of antioxidants.

Carotenoids and tocopherols are the most important antioxidants that give protection against the damages of $^1O_2$ (Khorobrykh et al., 2020). Carotenoids are found either bound to the photosynthetic machinery or free in the thylakoid membrane (Pinnola & Bassi, 2018). For example, the core of PSII binds several β-carotenes, while LHCs bind xanthophylls in the close proximity of chlorophylls (Umena et al., 2011). Bound carotenoids play an important role in the NPQ, thus protecting organism from the formation of $^3P_{680}$, and possible further damages caused by $^1O_2$ (Khorobrykh et al., 2020). In the case of $^1O_2$ itself, the detoxification by the carotenoids occurs through physical quenching (Khorobrykh et al., 2020). In this physical quenching, carotenoids interact with $^1O_2$ through charge-transfer mechanism, which results in the formation of ground-state O_2 and triplet-state carotenoid (Schweitzer & Schmidt, 2003). Triplet-state carotenoid returns to its ground-state by dissipating the excitation energy via non-radiative transformation resulting in heat. In addition to the quenching, carotenoids can scavenge $^1O_2$ through oxidation (Pinnola & Bassi, 2018). Oxidation products of carotenoids are suggested to work as signaling molecules in $^1O_2$-dependent signaling inside the cell (Khorobrykh et al., 2020). Tocopherols are another important antioxidant acting against $^1O_2$ (Khorobrykh et al., 2020). In contrast with the carotenoids, tocopherols are free-form antioxidants that are not bound to photosynthetic machinery. This makes them important antioxidants inside the thylakoid membrane, acting against the $^1O_2$ that has escaped from its evolving site. Detoxification mechanisms are similar to carotenoids, where tocopherols quench $^1O_2$ through physical deactivation via charge-transfer mechanism (Khorobrykh et al., 2020). It is also shown that tocopherols act as chemical scavengers against $^1O_2$ (Krieger-Liszkay & Trebst, 2006). α-tocopherol is a part of ascorbate-glutathione cycle (Foyer-Halliwell-Asada pathway), scavenging the $^1O_2$ in the lipid phase but also in the stroma (Foyer et al., 2008). Other

potential compounds suggested to be involved in the detoxification of $^1O_2$ are ascorbate, glutathione, flavonoids, unsaturated fatty acids, and plastoquinol (Pinnola & Bassi, 2018).

1.5 Photoinhibition

As a source of life and energy in photosynthesis, light can also paradoxically cause severe damage to photosynthetic machinery. Photoinhibition is a phenomenon where light induces irreversible damage to a photosynthetic apparatus, leading to a loss of photosynthetic activity. In photoinhibition, activity is lost in the O_2 evolution and electron transport activity. It is of great importance to define the term photoinhibition, as in literature, the term is used to describe the downregulatory nature of the processes in photosynthesis in and beyond the saturating light. In these conditions NPQ mainly protects photosynthetic machinery from excess light (see chapter 1.5.5), while the rate of photosynthesis decreases, causing similar response compared to photoinhibition (Tyystjärvi, 2013). The regulatory nature of this phenomenon is underlined, when the light conditions are lowered back to saturating light, causing increase in the rate of photosynthesis. However, it should be noted that the further investigations of this phenomenon in microalgae has shown to be an artefact of fluorescence measurement, which indicates to an unknown quenching mechanism within PSII in addition to NPQ (Havurinne et al., 2019). In this study, the term photoinhibition is used strictly to describe the irreversible light-induced damage to photosynthetic machinery that needs protein synthesis in order to recover.

The damage of photoinhibition targets both reaction centers, causing structural changes and a loss of photosynthetic activity. Even though photoinhibition is a known phenomenon at both reaction centers, the major site of the damage is located at PSII complexes. Compared to PSI complexes, PSII complexes are more sensitive to light and light-induced damage. PSI photoinhibition takes place under severe conditions where electron transport becomes uncontrolled, leading to the formation of ROS that are regarded as damaging agents in PSI photoinhibition (Sonoike, 2011; Tiwari et al., 2016). In PSI photoinhibition, electron flow from PSII complexes plays a crucial role, being a prerequisite to PSI photoinhibition (Sonoike, 2011). It is suggested that photoinhibition of PSII complexes serves as a protective mechanism to PSI, as the damage to PSI complexes is permanent and more costly (Sonoike, 2011; Tikkanen et al., 2014). In this study, photoinhibition is illustrated from the point of view of PSII complexes.

Photoinhibition of PSII complexes has been an extensively studied topic for a several decades (for review, see for example Vass, 2012; Tyystjärvi, 2013). It is an ordinary phenomenon known to happen all the time in all light intensities (Tyystjärvi & Aro, 1996). The inhibitional side of photoinhibition is apparent when repairing protein synthesis can't keep up with the rate of damage. This leads to an observed decrease in photosynthetic activity. In PSII complexes, photoinhibition leads to a loss of O_2 evolution and electron transfer activity. Light induces damage that alters the structure of reaction centers in PSII complexes. As a result of photoinhibition, the PSII reaction center undergoes a sequence of reactions, where the D1 protein is degraded and replaced with a new one (Nath et al., 2013). This sequence of reactions is known as the PSII repair cycle. It enables photosynthetic organisms to maintain their photosynthetic activity despite the light-induced damage caused by photoinhibition.

Besides the correlation between the light intensity and rate constant of photoinhibition, it is known that photoinhibition follows first-order reaction kinetics (Sarvikas et al., 2010; Tyystjärvi, 2013), which means the reaction rate of photoinhibition is directly proportional to the concentration of one reactant. In other words, photoinhibition is a one-step reaction that causes the inactivation of PSII. The quantum yield of photoinhibition is approximately 10^{-7} in visible light (Tyystjärvi & Aro, 1996), meaning every tenth million absorbed and photosynthetically active photons will cause an inactivation of PSII. Action spectrum of photoinhibition shows strong increase towards ultraviolet light, starting from the blue-green region (Jones & Kok, 1966; Hakala et al., 2005; Ohnishi et al., 2005). In this region manganese ions of OEC are the only possible components of PSII to cause this kind of spectral response, therefore suggesting their pivotal role in photoinhibition at this range (Hakala et al., 2005). Another peak is observed at the red light region (Jones & Kok, 1966), suggesting the involvement of chlorophylls as photoreceptors in photoinhibition at this range (Tyystjärvi, 2013). Recent studies have also confirmed that temperature dependency of photoinhibition is positive (Tyystjärvi et al., 1994; Mattila et al., 2020; Mattila et al., 2023), even though contrasting and varying results have been represented (Tyystjärvi, 2013).

Even though photoinhibition of PSII complexes is an extensively studied phenomenon, the exact molecular mechanism, or molecular mechanisms, in visible light are yet to be known (Vass, 2012; Tyystjärvi, 2013). The debate remains about the contribution of different mechanisms to the photoinhibition of PSII complexes. In addition, the distribution of these mechanisms in the spectrum of visible light is not clearly understood. It is also suggested that in the range of visible light, photoinhibition could have three parallel mechanisms contributing

to the overall inactivation of PSII (Mattila et al., 2023). In ultraviolet light, it is a widely accepted consensus that photoinhibition is caused through manganese ions of OEC (Vass, 2012). In the current literature, theories of photoinhibition are generally categorized into three groups based on the site or reaction pathway responsible for the initial light-induced inactivation of PSII.

1.5.1 Long lived P_{680}^+ (or $TyrZ^+$•) acting as a damaging agent in photoinhibition

P_{680}^+ is a strong oxidant capable of acting as a damaging agent in photoinhibition of PSII complexes (Vass, 2012; Tyystjärvi, 2013). Acting as an oxidant, long lived P_{680}^+ could cause crucial modifications in the structure of PSII reaction center (Jegerschlöd et al., 1990; Anderson et al., 1998), leading to inactivation of PSII reaction center and a decrease in the overall photosynthetic activity. Besides P_{680}^+, it is also suggested that long lived $TyrZ^+$• could act as a damaging agent in the similar manner (Jegerschlöd et al., 1990). The formation of aforementioned highly oxidative compounds are linked to the classical donor-side mechanism of photoinhibition.

In the classical donor side mechanism, the electron transfer activity is inhibited or lost at the luminal side of PSII, leading to formation of long lived P_{680}^+ or $TyrZ^+$• (Tyystjärvi, 2013). This could be caused by "misses" taking place at the OEC. In these "misses", S-state transition fails to proceed after the absorption of photon, causing a stoppage in the electron flow from OEC to P_{680}. In other words, "misses" cause a situation where the OEC fails to reduce P_{680}^+ or $TyrZ^+$•, enabling them to cause oxidative damage and photoinhibition trough donor-side mechanism. "Misses" at the OEC are constant phenomenon (Pham et al., 2019), representing the reaction equilibria between S-state transitions and recombination pathways in normally active and functioning PSII (Mattila et al., 2023). Besides the involvement of "misses" in donor-side mechanism, it has been suggested that misses play pivotal role in the formation of $^1O_2$ (Mattila et al., 2023).

Facts speaking for P_{680}^+ (or $TyrZ^+$•) acting as damaging agents in photoinhibition are the normally occurring "misses" at the OEC and its independency from O_2 in anaerobic conditions (Vass et al., 1992). Also the action spectrum of photoinhibition supports the donor-side mechanism in the red light region, where the chlorophylls in PSII antenna can act as a photoreceptor of photoinhibition in classical donor-side mechanism.

1.5.2 Manganese mechanism in photoinhibition

In manganese mechanism, Mn ions act as a photoreceptor of photoinhibition (Hakala et al., 2005). Photons absorbed by Mn ions at the OEC lead to the excitation of Mn ions, which in turn leads to their release, making the OEC inactive and the PSII inhibited (Hakala et al., 2005; Tyystjärvi, 2013). After the irreversible inactivation of OEC, additional damage to PSII is caused in similar manner as in donor-side mechanism, where P_{680}^{+} or $TyrZ^{+}\bullet$ act as damaging agents. Manganese mechanism of photoinhibition has also been referred as a two-step mechanism (Ohnishi et al., 2005). The first step of the mechanism involves the inactivation of OEC through light-absorption of Mn ion, whereas the second step involves the further damage to PSII reaction center through formation of P_{680}^{+} or $TyrZ^{+}\bullet$. When illustrating this type of two-step mechanism, it is of great importance to underline the first-order reaction kinetics of photoinhibition. First-order kinetics of photoinhibition indicate that light-absorption and consequent release of Mn ion from OEC is irreversible reaction inactivating PSII. Additional damage caused by P_{680}^{+} or $TyrZ^{+}\bullet$ is then taking place at an already inactive PSII, or at another functional PSII reaction center (Tyystjärvi, 2013).

Several facts speak in advance for manganese mechanism in photoinhibition. First of all, observed action spectrum of photoinhibition gives strong indication of the involvement of Mn ions acting as photoreceptors in photoinhibition even in the region of visible light (Hakala et al., 2005; Ohnishi et al., 2005), despite the peak at the red light region pointing towards the involvement of chlorophylls causing photoinhibition. Another important factor pointing towards manganese mechanism is that it could act separately from electron transport chain. The independence of antenna size, the direct proportionality between light intensity and the rate constant, minor and inefficient protection by NPQ, and the similarity of photoinhibition caused by short flashes and continuous illumination, indicate that photoinhibition is not dependent of the electron transport reactions in PSII (Tyystjärvi, 2013). Finally, photoinhibition is known to occur also in anaerobic conditions (Vass et al., 1992; Mattila et al., 2023), which suits also for manganese mechanism working independently of O_2.

1.5.3 Singlet oxygen acting as a damaging agent in photoinhibition

$^1O_2$ formed at the PSII reaction centers could act as another damaging agent in photoinhibition under visible light. In the PSII, the formation of $^1O_2$ is linked to excited triplet-state chlorophylls, which in hand are evolved through spontaneous spin conversion of excited chlorophyll, or charge recombination pathways (Vass, 2012; Tyystjärvi, 2013). In the context of photoinhibition, charge recombination reactions leading to formation of excited triplet-state chlorophyll, and the evolution of $^1O_2$ later on, are referred to as the charge recombination mechanism in photoinhibition (Keren et al., 1997). In addition and besides with the other ROS, $^1O_2$ could be linked to inhibition of PSII repair cycle, where it oxidizes translational factors and therefore inhibits the synthesis of a new D1 protein (Nishiyama et al., 2004, Tyystjärvi, 2013).

Charge recombination mechanism in photoinhibition is solely dependent on electron transport in PSII reaction center. In the charge recombination mechanism, the formation of $^3P_{680}$ is associated with either to $S_{2/3}Q_B^- \rightarrow S_{1/2}Q_B$ or $S_{2/3}Q_A^- \rightarrow S_{1/2}Q_A$ recombination (Vass, 2011; Tyystjärvi, 2013), or the recombination of $[P_{680}^+Q_A^-]$ (Mattila et al., 2023). The recombination reactions $S_{2/3}Q_B^- \rightarrow S_{1/2}Q_B$ or $S_{2/3}Q_A^- \rightarrow S_{1/2}Q_A$ leading to formation of $^1O_2$ have been suggested to prevail in weak light (Keren et al., 1997), due to their extremely slow reaction kinetics. On the other hand, the recombination of the primary charge pair $[P_{680}^+Pheo^-]$ could take place multiple times before the secondary electron transport to Q_A. The formation of $^3P_{680}$ is suggested to be enabled through this pathway especially when Q_A is in its reduced state in high-light conditions (Vass & Styring, 1993). In other words, the formation of $^3P_{680}$ through $[P_{680}^+Pheo^-]$ in high-light conditions is enabled when the reaction centers are closed. However, the effect of photoinhibition in NPQ-less mutants, where Q_A is more often in its reduced form, was found to be much lower than expected (Sarvikas et al., 2006). NPQ is a way for photosynthetic organism to protect itself from excess light-energy. In this mechanism, absorbed light-energy by chlorophyll is transformed into heat before it reaches to reaction center to cause possible harm. This suggests the minor role of $^1O_2$ in photoinhibition, when it has evolved through the primary charge pair $[P_{680}^+Pheo^-]$ recombination pathway.

The recombination of $[P_{680}^+Q_A^-]$ is enabled when OEC fails to provide electrons to P_{680}^+. These failures of OEC to reduce P_{680}^+ are called “misses”, which occur regularly at OEC in photosynthetic electron transport. The time constant of the recombination of $[P_{680}^+Q_A^-]$ is 100–200 µs (Renger & Wolff, 1976), whereas the time constants for S-state transitions vary from 300 µs to 2 ms at their slowest (Klauss et al., 2012). However, misses occur because the OEC

has a special S-state, where the advancement of S-state is so slow or not existent that the $[P_{680}^{+}Q_A^{-}]$ recombines, not because the recombination of $[P_{680}^{+}Q_A^{-}]$ occasionally wins the competition with the normal S-state transition (Pham et al., 2019; Mattila et al., 2023). Recent study by Mattila et al. (2023) suggested that evolution of $^1O_2$ is linked to "miss"-associated recombination pathways, playing a significant role in photoinhibition in the range of visible light, especially while moving towards longer wavelengths.

Several facts also speak in advance for $^1O_2$ to act as a damaging agent in photoinhibition. Peak in the red light region of the action spectrum of photoinhibition indicates PSII antenna or uncoupled chlorophylls to act as photoreceptors in photoinhibition. In the case of chlorophylls in PSII antenna, this would lead to intersystem crossing and the formation of $^1O_2$ to act as a damaging agent in photoinhibition. Uncoupled chlorophylls acting as photoreceptors in photoinhibition would partly explain the relatively weak protection offered by NPQ (Santabarbara et al., 2001). Uncoupled chlorophylls producing $^1O_2$ would also explain photoinhibition working independently from the electron transfer reactions. It is also suggested that $^1O_2$ produced by sensitized cytochromes and iron-sulfur centers could produce $^1O_2$ independently from electron transport in PSII (Jung & Kim, 1990). Recent finding of "miss"-associated $^1O_2$ production fulfills the picture of light response further. The results of using compounds enhancing the production of $^1O_2$, and the damage of PSII vary (Tyystjärvi, 2013). Similar kinds of results have been found while using quenchers and scavengers that should protect PSII from $^1O_2$. To conclude, PSII is known to be the main source of $^1O_2$ in the photosynthetic apparatus, therefore making $^1O_2$ suitable for acting as a possible damaging agent in photoinhibition.

1.5.4 PSII repair cycle

Damaged PSII reaction centers get repaired in so called PSII repair cycle. The core function of this cycle is to degrade D1 protein in the damaged PSII reaction center and replace it with newly synthetized one (for review, see Nath et al., 2013; Järvi et al., 2015). With the help of the PSII repair cycle, photosynthetic organisms are able to maintain their photosynthetic activity, even in high-light conditions. The PSII repair cycle is also partly responsible for the rate of decrease in photosynthetic activity due to photoinhibition in the physiological conditions. That is to say, if the net accumulation of damaged and inactive PSII complexes is faster than their repair cycle, this results in the decrease of photosynthetic activity. This should also be taken into account

while observing the light-induced irreversible damage caused by photoinhibition. In order to separate the PSII repair cycle and damage caused by photoinhibition from one another, lincomycin is commonly used to block the protein synthesis of D1 protein. This stops the PSII repair cycle from performing its functions, so that the damage caused by photoinhibition can be observed. Lincomycin inhibits bacterial translation, which makes it effective against the synthesis of the D1 protein, as this protein is coded by the chloroplast genome in plants and algae. In cyanobacteria, lincomycin blocks translation overall. The repair cycle has also been found to be sensitive to environmental stress conditions that lead to the formation of ROS (Nath et al., 2013; Tyystjärvi, 2013). Several different ROS, such as H_2O_2, $^1O_2$ and $O_2^{\bullet -}$, are known to inhibit the synthesis of D1 protein (Nishiyama et al., 2004; Jimbo et al., 2013). H_2O_2 and $^1O_2$ are also known to cause fragmentation of the D1 protein (Miyao et al., 1995).

The PSII repair cycle could be said to start with photoinhibition, which in turn leads to the monomerization of the PSII dimer. Monomerization of the PSII dimer could be considered as a prerequisite to the cycle. In plants, this results in the movement of damaged PSII units from grana stacks towards the non-appressed stromal thylakoids or grana margins (Aro et al., 2005), where D1 protein could be easily degraded and replaced. This could be considered as another prerequisite to PSII repair cycle to work. In cyanobacteria, it is suggested that damaged PSII complexes move to special regions meant for PSII repairing cycle (Sacharz et al., 2015). Phosphorylation and dephosphorylation of PSII core proteins is suggested to facilitate the movement of the PSII complexes towards the non-appressed areas, and vice versa (Nath et al., 2013). Besides the phosphorylation and dephosphorylation, the lateral heterogeneity of thylakoid membrane structures plays an important role in the movement of protein complexes.

Degradation of D1 protein is done by chloroplast proteases Deg1 and FtsH. Before the degradation, PSII complex is disassembled by the release of CP43, OEC proteins, and another smaller sub-unit yet to be identified (Järvi et al., 2015). After the disassembly of PSII, Deg1 and FtsH proteases degrade D1 protein from both sides of thylakoid membrane (Nath et al., 2013; Järvi et al., 2015). It is also suggested that in addition of Deg1 and FtsH proteases, also other housekeeping proteases are needed for the full degradation of D1 protein (Nath et al., 2013). After the degradation, the D1 protein is replaced with a newly synthetized copy of a functional D1 protein. In plants, algae, and cyanobacteria, the D1 protein is coded by the *psbA* gene family. Among the several steps, de novo synthesis could be argued to be the most important step to terminate the PSII repair cycle, enabling the reassembly of functional PSII

complex (Nath et al., 2013). After the reassembly, a functional PSII complex is reassembled and moved to grana thylakoids to maintain its functions.

1.5.5 Protective mechanisms against excess light energy

While the PSII repair cycle could be considered a photoprotective mechanism or a response to light-induced damage, photosynthetic organisms have also evolved other protective mechanisms and responses to excess light energy. With the help of these, organisms acclimate to fluctuating and severe light conditions. Slow responses to changing light-conditions are, for example, changes in phyllotaxis or changes in the spatial arrangement of chloroplasts inside the cell. Changes in gene regulation and expression due to prevailing light conditions could also be considered slow responses. Faster responses to changing light conditions are achieved through NPQ and state transitions. Along with the PSII repair cycle, NPQ is mainly responsible for the fast protection against excess light energy. State transitions could be considered as a fast adaptation mechanism to changing light conditions, rather than a protective mechanism.

Already mentioned NPQ dissipates excess light energy as heat. Between organisms, the mechanisms of NPQ vary greatly. In plants, NPQ could act in three different pathways, where the quenching of excess light energy is made either through energy dependent pathway (q_E), state transition dependent pathway (q_T), or photoinhibition dependent pathway (q_I) (Quick & Stitt, 1989). Out of the three, the q_E pathway is considered to be the most important one (Wraight & Crofts, 1970). This pathway works through PsbS protein dimers, which monitor changes in lumenal pH (Li et al., 2000). The PsbS protein is a thylakoid membrane embedded protein that also acts as a subunit of the PSII complex. Once the lumen pH decreases, protonation of PsbS dimers enables the q_E pathway to function. The actual molecular mechanism of quenching in the q_E pathway is not fully understood. Besides the PsbS, involvement of the xanthophyll cycle has been shown to play role in the q_E pathway (van Amerongen & Chmeliov, 2020). Regardless of the pathway, NPQ lowers the number of excited singlet-state chlorophylls and, as a consequence, lowers the number of triplet-state chlorophylls, which are capable of producing $^1O_2$.

In cyanobacteria, NPQ takes place at the core of the phycobilisome and involves the orange carotenoid protein (OCP) binding a single xanthophyll as a crucial part of the process (El Bissati et al., 2000; Niyogi & Truong, 2013). In this NPQ process, OCP absorbs blue-green light and

undergoes a conformational change, converting OCP to an active form (Wilson et al., 2008). Active form of OCP binds to a phycobilisome to quench the excess excitation energy (Niyogi & Truong, 2013). At the molecular level, the quenching mechanism involves a charge (Tian et al., 2011), or energy (Berera et al., 2012), transfer reaction from an excited bilin pigment located at the core of the phycobilisome to the carotenoid of OCP (Niyogi & Truong, 2013).

In state transitions, the organism compensates for an unequal energy distribution between PSII and PSI. State transitions are important especially in fluctuating light conditions, where exposure to severe light conditions can be momentary. The two photosystems work with distinct absorption characteristics and action spectra, where PSII absorption is located in the blue and red light regions, and PSI has absorption peaks in blue and red as well as in the far-red light region (Minagawa, 2011). In plants, within the range of visible light, wavelengths favoring PSII are located at 460–500 nm in the blue light region, 560–570 nm in the green light region, and 650–660 nm in the red light region (Mattila et al., 2020). On the contrary, wavelengths favoring the PSI are located at 420–440 nm in the blue light region, 520 nm at the green light region, 630 nm in the red light region, and 680–690 nm in the far-red light region (Mattila et al., 2020). Under natural light conditions, sun light tends to favor PSI to some extent. In addition, in natural conditions light quality and quantity tend to be fluctuating over time. An imbalance of excitation energy between two photosystems can lead to a decrease in photosynthetic activity and possible light-induced damage.

In plants and green algae, state transitions operate through phosphorylation and dephosphorylation of LHCII proteins. To put it simply, light conditions favoring PSII induce the phosphorylation of LHCII proteins resulting in a “state 2” transition, where phosphorylated LHCII proteins detach from PSII and attach to PSI (Tikkanen et al., 2011). The phosphorylation of LCHII proteins is catalyzed by the Stt7/STN7 kinase (Bonardi et al., 2005). On the contrary, light conditions favoring PSI induce the dephosphorylation of LHCII proteins resulting in a “state 1” transition in which LHCII proteins attach back to PSII complexes. Dephosphorylation of LHCII is catalyzed by the TAP38/PPH1 phosphatase (Shapiguzov et al., 2010). Light conditions also induce changes in the redox state of the plastoquinone pool, which affects the activity of the Stt7/STN7 kinase (Vener et al., 1997). In the more reduced state of the plastoquinone pool, plastoquinol binds to Cytb_6f binding site activating the Stt7/STN7 kinase (Vener et al., 1997; Minagawa, 2011). TAP38/PHH1 phosphatase is always active (Minagawa, 2011).

In cyanobacteria the mechanisms of state transitions are less known. Rapid diffusion and change in spatial arrangement of phycobilisome is suggested to cause state transition and redistribute energy between PSII and PSI (Mullineaux & Allen, 1988). The other suggested mechanism for state transitions in cyanobacteria is the "spillover" of excitation energy from PSII to PSI (Bhatti et al., 2020). To fulfil the picture of state transitions in cyanobacteria, also the increased excited-state quenching in the reaction center of PSII is proposed to balance the excitation energy difference between the two photosystems (Ranjbar Choubeh et al., 2018).

1.6 Aims of the study

Aims of the thesis can be divided into two different compartments. Firstly, the photoinhibition was measured under different circumstances by varying temperature and light conditions. The goal was to measure the possible temperature dependency of the rate constant of photoinhibition (k_{PI}) in red and blue light. This was done *in vitro* and *in vivo*. Isolated pumpkin (*Cucurbita maxima* L.) thylakoids were used for *in vitro* experiments, while *Synechocystis* sp. PCC 6803 GT-T and *Synechocystis* sp. PCC 6803 ΔsigCDE were used for *in vivo* experiments.

The second intention of this study was to investigate the potential involvement of $^1O_2$ in photoinhibition under the aforementioned conditions by varying the reaction medium. This was done by using D_2O as a solvent in photoinhibition treatments with isolated pumpkin thylakoids, and comparing the obtained results to the corresponding ones in water based medium. D_2O prolongs the lifetime of $^1O_2$, enabling it to act as a damaging agent more extensively. The other method used for testing the involvement of $^1O_2$ in this study, was the use of the ΔsigCDE mutant strain. The ΔsigCDE strain lacks three group 2 σ factors, which enables it to obtain a high carotenoid content inside the cell (Pollari et al., 2011; Hakkila et al., 2013). Carotenoids are important antioxidants in all living cells acting as important quenchers and scavengers of $^1O_2$. Thus, the ΔsigCDE strain is expected to have better resistance against the harms of $^1O_2$ compared to the control stain. In photoinhibition, the involvement of $^1O_2$ has been suggested to become more important while moving towards red light region and higher temperatures (Mattila et al., 2023).

2 Materials and methods

2.1 Organisms and growth conditions

Isolated pumpkin (*Cucurbita maxima* L.) thylakoids, the glucose-tolerant *Synechocystis* sp. PCC 6803 GT-T control strain (CS), and a σ factor inactivation stain ΔsigCDE were used for the photoinhibition experiments. Pumpkin was grown at 23 °C, in long day circumstances of 16 h of illumination and 8 h of darkness, with photosynthetic photon flux density (PPFD) of 200 µmol m^{-2} s^{-1}. For experiments, full grown and healthy leaves were used for thylakoid membrane isolation. Thylakoid membranes were isolated by grinding pumpkin leaves in isolation buffer (40 mM HEPES-KOH (pH 7.4); 0.3 M sorbitol; 10 mM $MgCl_2$; 1 mM Na-EDTA; 1 M betaine monohydrate; 1 % bovine serum albumin), and then filtering the ground suspension through Miracloth™ (Merck, Germany). Ground and filtered suspension was centrifuged at 2500 x g for 4 min at 4 °C. After centrifugation, the pellet was resuspended in osmotic shock buffer (10 mM HEPES-KOH (pH 7.4); 5 mM sorbitol; 5 mM $MgCl_2$) and centrifuged once again at 2500 x g for 4 min at 4 °C. After centrifugation, the pellet was resuspended in storage buffer (10 mM HEPES-KOH (pH 7.4); 0.5 M sorbitol; 10 mM $MgCl_2$; 5 mM NaCl) and flash frozen in liquid nitrogen before storing isolated thylakoids at -75 °C until use.

Synechocystis sp. PCC 6803 GT-T and ΔsigCDE cells, from a long-term storage of -80 °C, were maintained on BG-11 agar plates (Rippka et al., 1979) supplied with 20 mM HEPES-NaOH (pH 7.4) in continuous illumination at the PPFD of 40 µmol m^{-2} s^{-1}; 32 °C; in ambient CO_2 of 0.04%. ΔsigCDE BG-11 agar plates were also supplied with 50 µg ml^{-1} kanamycin; 20 µg ml^{-1} spectinomycin; 10 µg ml^{-1} streptomycin; and 10 µg ml^{-1} chloramphenicol. A few days before the experiments, *Synechocystis* cells were transformed to liquid cultures without antibiotics (30 ml cell culture in a 100-ml Erlenmeyer flask) and A_{730} was set to 0.06. Cells were grown to A_{730} of ~0.6–0.8 in growth conditions as previously described, with shaking at 90 RPM.

2.2 Photoinhibition treatments

Photoinhibition treatments were made in four different temperatures (10 °C; 22 °C; 32 °C or 40 °C) with two different wavelengths, in the region of blue or red light. White light used for the

illumination was obtained from a 1000 W (Sciencetech, London, ON, Canada) high-pressure Xenon lamp, and short-pass or long-pass filters were used for obtaining desired wavelengths. For the blue light region, a 450 nm short-pass filter (LS-450; Corion, Holliston, MA, USA) was used, whereas for the red light region a 600 nm or, as indicated, a 650 nm long-pass filter (LL-600 or LL-650; Corion, Holliston, MA, USA) as used. For the treatments 6 ml samples were made. Before the illumination all samples were incubated for 10 min in the dark in the reaction cuvette. All of samples were gently mixed during the photoinhibition treatments with a magnetic stirrer bar.

For the pumpkin thylakoids, photoinhibition treatments were made in photoinhibition buffer (40 mM HEPES-KOH (pH 7.4); 1 M betaine monohydrate; 0.33 mM sorbitol; 5 mM NaCl; 5mM Mg_2Cl) for 60 min. Chlorophyll content of thylakoid membranes was adjusted to 20 µg Chl ml^{-1} for the treatments. PPFD was set to 500 µmol m^{-2} s^{-1} in the blue light region or to 1000 µmol m^{-2} s^{-1} in the red light (LL-650 filter) region (Fig. 1). Energy spectra for the used filters were measured with STS-VIS (Ocean Optics, Orlando, FL, USA).

For the *Synechocystis* strains, cells were concentrated to a theoretical optical density of 1.4 at 730 nm before the photoinhibition treatments. Concentration was done by centrifuging cells at 3000 x g for 1 min at room temperature, and then by resuspending the pellet to fresh BG-11. Photoinhibition treatments were made in BG-11 with 0.4 mg ml^{-1} of lincomycin, where lincomycin was added to cells right before the treatments. PPFD was set to 350 µmol m^{-2} s^{-1} in the blue light region or to 1000 µmol m^{-2} s^{-1} in the red light (LL-600 filter) region (Fig. 1). In blue light, the length of the treatment was 60 min, whereas in red light, the length of the treatment was 90 min.

Treatments in the dark reaction system under otherwise identical conditions were done for pumpkin thylakoids and both *Synechocystis* strains. For the pumpkin thylakoids, dark treatments were done to determine the rate of dark inactivation of PSII under different temperatures. Dark treatments were done to the *Synechocystis* strains in order to determine the strain temperature responses in the reaction system, and to look for potential differences between the two strains that were used.

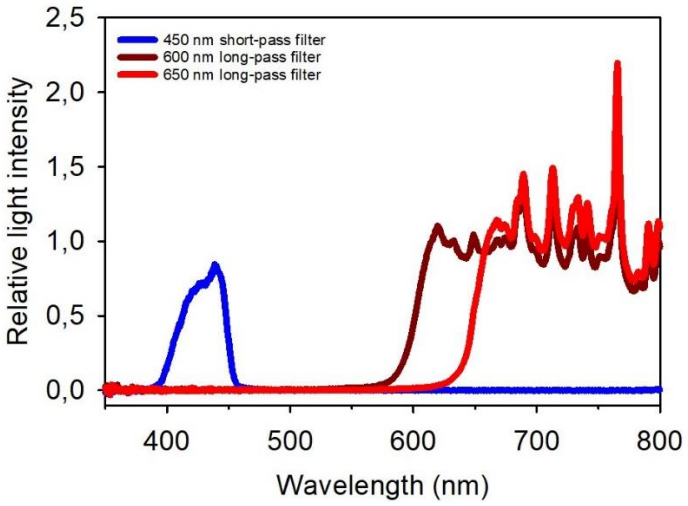

Figure 1. Energy spectra of used short- and long-pass filters in the combination of the Xenon lamp. Filters were used to obtain the light conditions of the photoinhibition treatments. 450 nm short-pass filter (blue line) (LS-450; Corion, Holliston, MA, USA) was used for the both model organisms, whereas 600 nm long-pass filter (dark red line) (LL-600; Corion, Holliston, MA, USA) was used for the *Synechocystis* sp PCC. 6803 and ΔsigCDE, and 650 nm long-pass filter (red line) (LL-650; Corion, Holliston, MA, USA) was used for isolated pumpkin (*C. maxima*) thylakoids.

2.3 Photoinhibition treatments in deuterium oxide

Photoinhibition treatments in deuterium oxide (D_2O) were done for pumpkin thylakoids in 10 °C and 32 °C in blue and red light regions, as previously described (see 2.2). Treatments were done in photoinhibition buffer in which H_2O was replaced with 99.9 % D_2O (Merck, Germany), and so the final D_2O content of the photoinhibition buffer was 95 %. As previously stated, dark treatments in the reaction system were made in identical conditions to determine the rate of dark inactivation of PSII in D_2O-based photoinhibition buffer.

2.4 Quantification of photoinhibition

2.4.1 Quantification of photoinhibition with oxygen electrode

Light-saturated O_2 evolution was measured from pumpkin thylakoids and *Synechocystis* cells before, during, and after the photoinhibition treatments. Quantification was made with an oxygen electrode (Hansatech, King's Lynn, UK) by measuring O_2 evolution at 0; 20; 40; and 60 min time marks, or at 0; 30; 60; and 90 min time marks for *Synechocystis* in red light. O_2 evolution measurements for the pumpkin thylakoids were made at 22 °C in PSII measuring

buffer (40 mM HEPES-KOH (pH 7.6); 0,33 mM sorbitol; 1 M betaine monohydrate; 5 mM NaCl; 5mM Mg_2Cl; 1 mM KH_2PO_4; 5 mM NH_4Cl) with 0.5 mM 2,6-diclhorobenzoquinone (DCBQ) acting as an artificial electron acceptor. Chlorophyll content for the pumpkin thylakoids was adjusted to 10 µg Chl ml^{-1}.

O_2 evolution measurements for the *Synechocystis* cells were made at 32 °C in BG-11, where the A_{730} was set to a theoretical 1.4. 0.5 mM DCBQ was used as an artificial electron acceptor alongside with 0.5 mM ferricyanide to keep DCBQ in its oxidized form.

2.4.2 Photoinhibition quantification with F_v/F_m fluorescence parameter

Alongside with oxygen electrode, the chlorophyll *a* fluorescence parameter F_v/F_m was measured from pumpkin thylakoids and *Synechocystis* cells before, during, and after the photoinhibition treatments. F_v/F_m parameter was measured with AquaPen AP-C 100 (Photon System Instruments, Brno, Czech Republic) at 0; 20; 40; and 60 min time marks, or at 0; 30; 60; and 90 min time marks for *Synechocystis* in red light by measuring the fluorescence after 5 min of dark incubation. Fluorescence measurements were made using 100 µl of treated sample diluted in 900 µl of photoinhibition buffer for pumpkin thylakoids and using 100 µl of treated sample diluted in 900 µl of BG-11 for *Synechocystis* cells. F_v/F_m parameter was used as an estimation of the relative numbers of functional PSII centers.

2.4.3 Photoinhibition rate constant calculations

Photoinhibition rate constant (k_{PI}) was calculated by using Sigmaplot (Systat Software Inc., Palo Alto, CA, USA) first-order reaction equation fitting, to quantify the rate at the loss of the O_2 evolution or the decrease of the F_v/F_m parameter. Two different kinds of first-order fits were made based on two or four free parameters. The rate constant of photoinhibition was also determined by using a fit based on only the first time points of the measurements by solving k_{PI} from the equation $y = y_0 e^{-k_{PI}t}$, where y is the O_2 evolution rate or the F_v/F_m fluorescence parameter at the first time mark after the illumination, y_0 is O_2 evolution rate or the F_v/F_m parameter before the illumination, and t is time, respectively. The final k_{PI} value for the thylakoids and *Synechocystis* strains was defined by subtracting the dark inactivation first-order reaction constant from the raw k_{PI} value. Statistical differences of k_{PI} values were analyzed through Student's *t* test, with two-tailed distribution and unequal variances.

3 Results

3.1 Photoinhibition of isolated pumpkin thylakoids deviates from first-order kinetics when quantified with oxygen evolution, both in water and D_2O

The reaction kinetics of photoinhibition treatments were analyzed in order to determine the rate constant k_{PI} for photoinhibition. Quantification of the rate constant k_{PI} enables comparison of photoinhibition under different conditions. To determine the temperature dependency of photoinhibition of PSII complexes either in red or blue light, isolated pumpkin thylakoids were illuminated in high light conditions at 10, 22, 32 and 40 °C. Thylakoids used in the treatments were isolated from the leaves of pumpkin plants (*C. maxima*) grown under moderate light conditions and at optimal temperature. Isolated thylakoids were stored at -75 °C until photoinhibition treatments. However, the photoinhibition treatments were only analyzed at 10, 22 and 32 °C. At 40 °C, the temperature conditions were simply too severe for thylakoids to maintain their functioning. The oxygen evolution and the F_v/F_m parameter were the two different parameters used in the quantification of photoinhibition. Both parameters were used to monitor the overall functioning of PSII complexes. According to both parameters, photoinhibition treatments led to a decrease in the overall photosynthetic activity of PSII. The light-induced decrease of PSII activity was fitted to first-order reaction kinetics with two free parameters according to equation $y = A_0 e^{-k_{PI} t}$, where y reflects the overall activity of PSII according to used parameter at certain time point, A_0 reflects the initial activity of PSII according to O_2 evolution rate or the F_v/F_m fluorescence parameter before the photoinhibition, t is time, and k_{PI} is the rate constant of photoinhibition to be determined.

With pumpkin thylakoids, photoinhibition treatments in both red and blue light led to a decrease in oxygen evolution rate, measured in saturating light. The decrease was found to deviate from first-order kinetics at all temperatures (Fig. 2AB). The deviation was most evident in first-order fits made from individual experiments, where particularly the loss of oxygen evolution rate at the first data point was found to be too steep compared to first-order fits (first-order fits from the individual experiments are not presented here). Here the first-order fits are presented from the averages of three different replicates, showing greater scatter in the bigger picture (Fig. 2AB).

Illumination of pumpkin thylakoids from the same photoinhibition treatments also led to a decrease in the F_v/F_m fluorescence parameter, which on the contrary was found to follow the first-order kinetics (Fig. 2CD). In the individual replicates, the decrease of the F_v/F_m parameter

was found to follow exactly the first-order kinetics. The fits presented here are made from averaged data, which lead to a slight scattering from the first-order kinetics (Fig. 2CD).

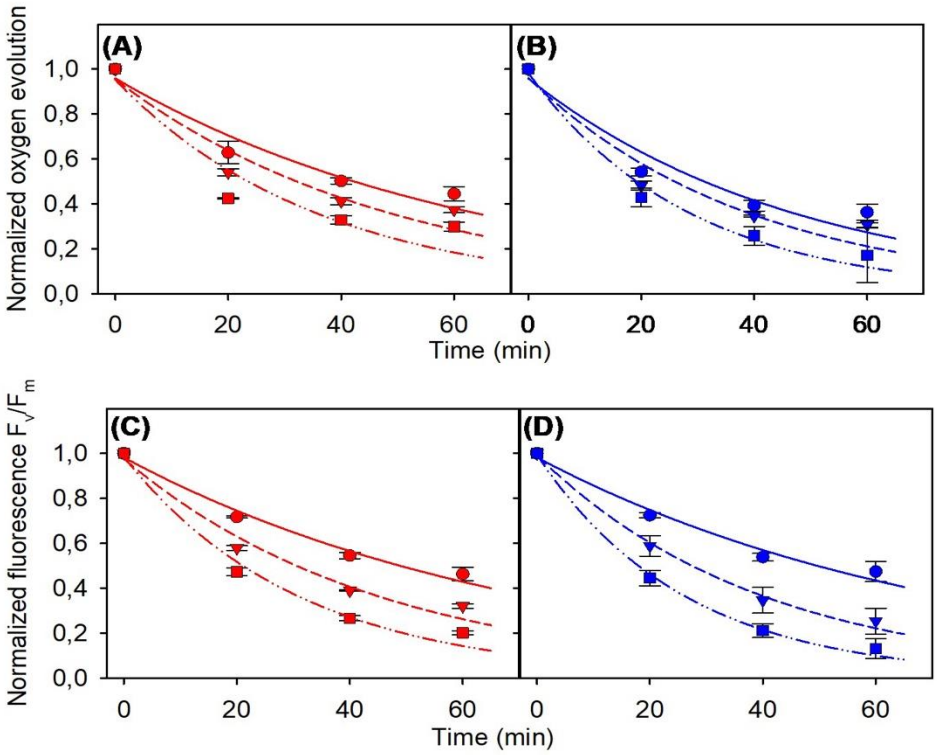

Figure 2. Photoinhibition of isolated pumpkin (*C. maxima*) thylakoids in water-based medium at 10 (circles, solid line), 22 (upward triangles, dashed line) and 32 °C (squares, dash-dotted line), in the red (**A, C**) and blue light (**B, D**). Quantification of the photoinhibition was done with the light-saturated oxygen evolution rate of PSII in water with 0.5 mM 2,6-diclhorobenzoquinone (**A, B**), or with chlorophyll *a* fluorescence parameter F_v/F_m (**C, D**). Oxygen evolution rate of PSII was measured with Clark-type oxygen electrode in saturating white light at 22 °C. The F_v/F_m parameter was measured after 5 min of dark incubation at room temperature. Quantification of photoinhibition with given parameters was made at 0, 20, 40, and 60 min time points during 60 min illumination. PPFD in the red light was 1000 µmol $m^{-2}s^{-1}$, whereas in the blue light PPFD was 500 µmol $m^{-2}s^{-1}$. Results are normalized to the PSII activity of oxygen evolution or to the F_v/F_m parameter before the illumination. The error bars indicate standard deviation from three biological replicates. Lines represent the best fit made into a first-order reaction.

To illustrate the possible involvement of $^1O_2$ in photoinhibition, the above-mentioned high-light treatments on isolated pumpkin thylakoids were repeated in D_2O at 10 and 32 °C. Quantification was made in a similar manner, with the same two parameters. As in water, photoinhibition treatments in D_2O lead to a gradual decrease in the overall activity of PSII (Fig. 3). The decrease

in PSII activity was fitted to first-order kinetics, according to equation $y = A_0 e^{-k_{PI} t}$ with A_0 and k_{PI} as free parameters.

Photoinhibition treatments in D_2O-based medium yielded similar kinds of results compared to water-based medium (Fig. 2), where deviation from the first-order kinetics were observed in the results quantified with oxygen evolution (Fig. 3AB). Deviation from first-order kinetics was most evident in the fits made from individual experiments. Quantification of the treatments with the F_v/F_m parameter yielded results, where the decrease of the parameter followed the first-order kinetics (Fig. 3CD). First-order fits presented here represent averaged data from three different replicates, which lead to a greater scattering of the data points from the first-order kinetics (Fig. 3CD).

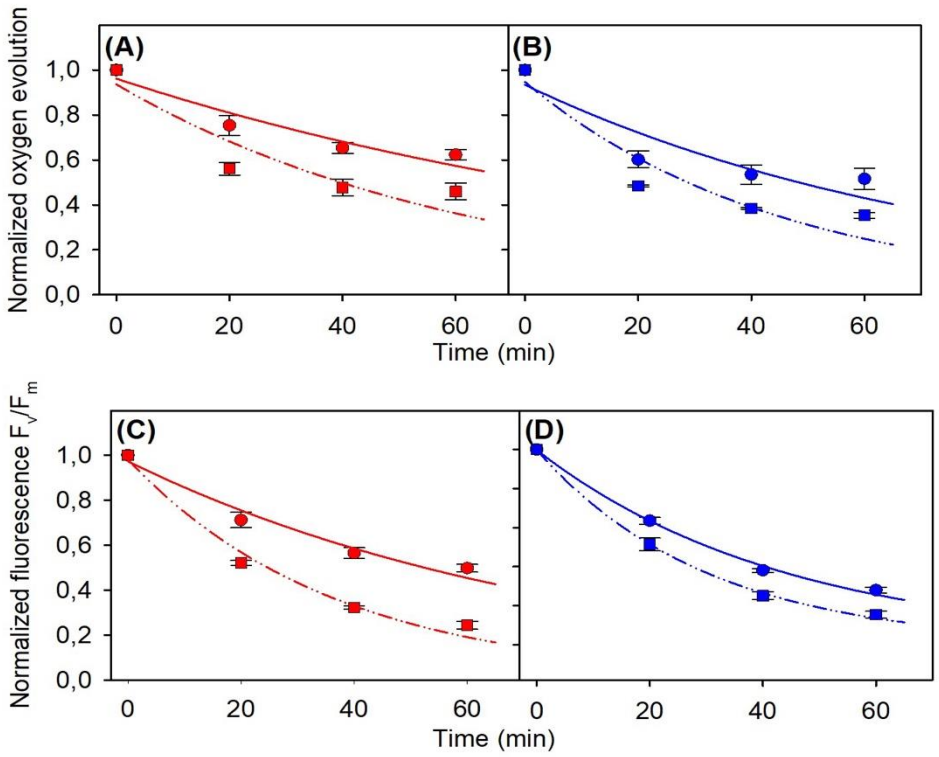

Figure 3. Photoinhibition of isolated pumpkin (*C. maxima*) thylakoids in D_2O-based medium at 10 (circles, solid line) and 32 °C (squares, dash-dotted line), in red (**A, C**) and blue light (**B, D**). Quantification of photoinhibition was done with light-saturated oxygen evolution rate of PSII in water with 0,5 mM 2.6-diclhorobenzoquinone (**A, B**), or with chlorophyll *a* fluorescence parameter F_v/F_m (**C, D**). Oxygen evolution rate of PSII was measured with Clark-type oxygen electrode in saturating white light at 22 °C. The F_v/F_m parameter was measured after 5 min of dark incubation at room temperature. Quantification of photoinhibition with given parameters was made at 0, 20, 40, and 60 min time points during 60 min illumination. PPFD in the red light was 1000 µmol $m^{-2}s^{-1}$, whereas in the blue light PPFD was 500 µmol $m^{-2}s^{-1}$. Results are normalized to the PSII activity of oxygen evolution or to the F_v/F_m parameter before the illumination. The error bars indicate standard deviation from three biological replicates. Lines represent the best fit made to a first-order reaction.

3.2 Deviation from the first-order kinetics was also observed in *Synechocystis* sp. PCC 6803 and ΔsigCDE when quantified with oxygen evolution

Besides the pumpkin thylakoids, the temperature dependency of photoinhibition either in red or blue light was studied also in *Synechocystis* sp. PCC 6803 GT-T (CS) and ΔsigCDE strains. This was done to ensure that the results are universal and not the property of the isolated system used in photoinhibition treatments. The ΔsigCDE strain was also used due to its resistance to photoinhibition (Hakkila et al., 2014), and particularly because of its presumed resistance to $^1O_2$, due to its high carotenoid contents inside the cell. Both *Synechocystis* strains were

illuminated in high-light conditions in the presence of lincomycin at 10, 22, 32 and 40 °C. Lincomycin was used to block the PSII repair cycle to measure the light-induced damage of photoinhibition. In addition, the red light treatments were prolonged from 60 min to 90 min so that the possible differences between two strains could be observed more clearly. Once again, the quantification of the treatments was made by using the oxygen evolution rate and the F_v/F_m fluorescence as parameters. Like in thylakoids, photoinhibition treatments led to a decrease in the overall photosynthetic activity of PSII, which was fitted to firs-order reaction kinetics according to the equation $y = A_0 e^{-k_{PI} t}$ (Fig. 4, Fig. 5). Again, two free parameters were used.

In both *Synechocystis* strains, photoinhibition treatments yielded similar kinds of results compared to isolated pumpkin thylakoids. Deviation from first-order kinetics could be observed from the results quantified with oxygen evolution (Fig. 4AB, Fig. 5AB), even though this was not the case at all temperatures. Deviations were most evident in first-order fits made from individual experiments (first-order fits from the individual experiments are not presented here). In the CS, deviation from first-order kinetics could be observed at 10 and 22 °C in red and blue light, at 32 °C in red light, and at 40 °C in blue light (Fig. 4AB). In the ΔsigCDE, deviation from the first-order kinetics could be observed at 22 and 40 °C in red and blue light, and at 32 °C in blue light (Fig. 5AB). Like in thylakoids, the deviation was most evident in the first data point from first-order fit, where the loss of oxygen evolving capability of PSII was too steep compared to first-order fits. Once more, first-order fits presented here are made of averaged data, which were calculated from three different replicates (Fig. 4, Fig. 5).

Interestingly, deviation from first-order kinetics was also found in both *Synechocystis* strains, when quantification of the treatments was made with the F_v/F_m parameter (Fig. 4CD, Fig. 5CD). In pumpkin thylakoids, a similar deviation was not observed in the F_v/F_m results (Fig. 4CD, Fig. 5CD). Deviations were most evident in the first-order fits made from individual experiments, where decrease of the F_v/F_m parameter was found to be too steep at the first data point compared to fitted data. In the CS, deviation from the first order kinetics was found at 10, 32, and 40 °C in red and blue light, and at 22 °C in red light (Fig. 4CD). In the ΔsigCDE, deviation was found at 10, 22, 32 °C in both light conditions, and at 40 °C in red light (Fig. 5CD). Compared to fits made with oxygen evolution, deviation from first-order kinetics was more subtle in the fits made with F_v/F_m parameter (Fig. 4, Fig. 5).

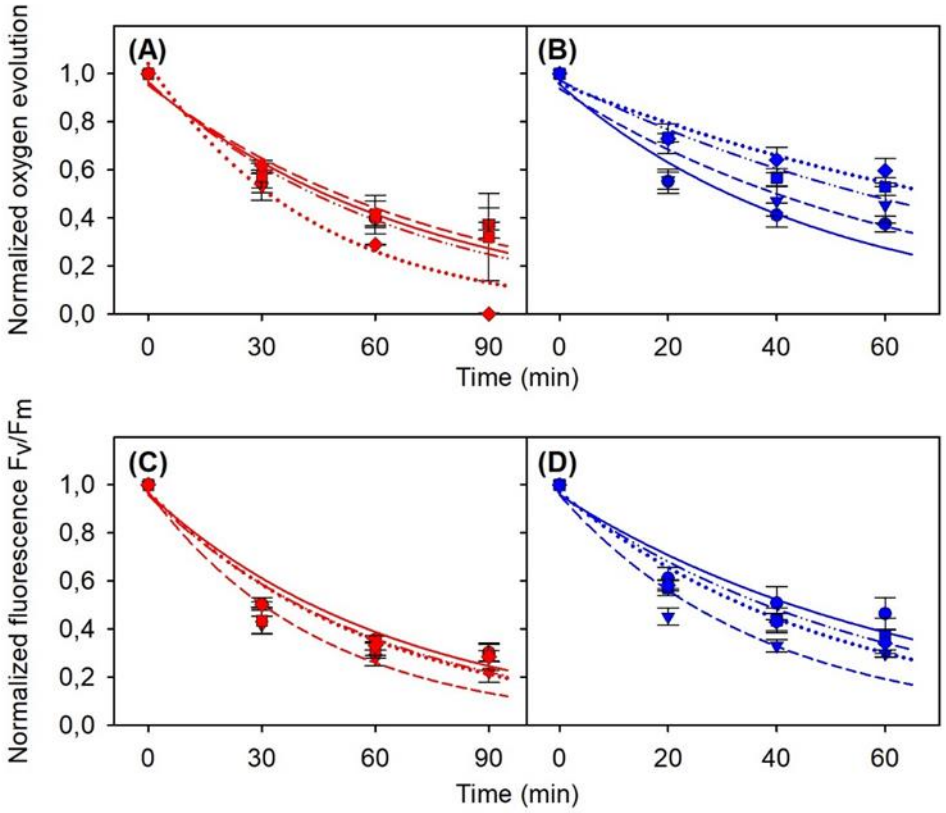

Figure 4. Photoinhibition of *Synechocystis* sp. PCC 6803 GT-T (CS) at 10 (circles, solid line), 32 (squares, dash-dotted line), and 40 °C (rhomb, dotted line), in red (**A, C**) and blue light (**B, D**). Quantification of the photoinhibition was done with light-saturated oxygen evolution rate of PSII in water with 0.5 mM 2,6-diclhorobenzoquinone and 0.5 mM ferricyanide (**A, B**), or with chlorophyll *a* fluorescence parameter F_v/F_m (**C, D**). Oxygen evolution rate of PSII was measured with Clark-type oxygen electrode in saturating white light at 32 °C. The F_v/F_m parameter was measured after 5 min of dark incubation at room temperature. Quantification of photoinhibition with given parameters was made at 0, 30, 60 and 90 min time points in the red light, and 0, 20, 40 and 60 min time points in the blue light during 90 or 60 min illumination. Lincomycin was used right before the treatments. PPFD in the red light was 1000 µmol $m^{-2}s^{-1}$, whereas in the blue light PPFD was 350 µmol $m^{-2}s^{-1}$. Results are normalized to the PSII activity of oxygen evolution or to the F_v/F_m parameter before the illumination. The error bars indicate standard deviation from three biological replicates. Lines represent the best fit made to a first-order reaction.

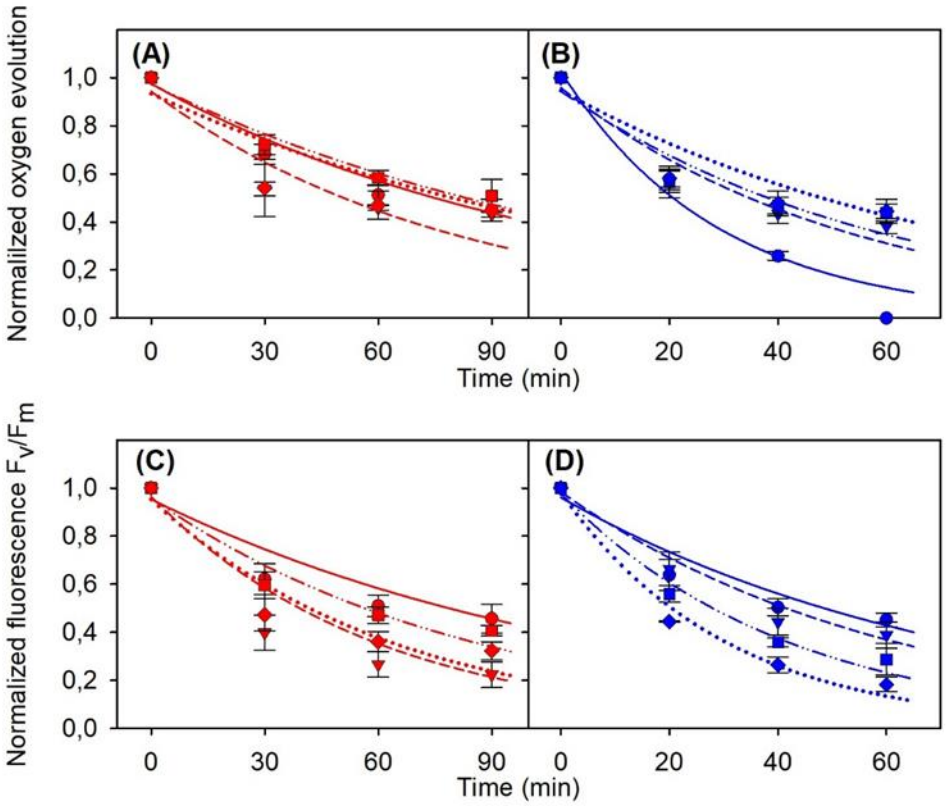

Figure 5. Photoinhibition of *Synechocystis* sp. PCC 6803 ΔsigCDE at 10 (circles, solid line), 32 (squares, dash-dotted line), and 40 °C (rhomb, dotted line), in red (**A, C**) and blue light (**B, D**). Quantification of the photoinhibition was done with light-saturated oxygen evolution rate of PSII in water with 0.5 mM 2,6-diclhorobenzoquinone and 0.5 mM ferricyanide (**A, B**), or with chlorophyll *a* fluorescence parameter F_v/F_m (**C, D**). Oxygen evolution rate of PSII was measured with Clark-type oxygen electrode in saturating white light at 32 °C. The F_v/F_m parameter was measured after 5 min of dark incubation at room temperature. Quantification of photoinhibition with given parameters was made at 0, 30, 60 and 90 min time points in the red light, and 0, 20, 40 and 60 min time points in the blue light during 90 or 60 min illumination. Lincomycin was used right before the treatments. PPFD in the red light was 1000 µmol $m^{-2}s^{-1}$, whereas in the blue light PPFD was 350 µmol $m^{-2}s^{-1}$. Results are normalized to the PSII activity of oxygen evolution or to the F_v/F_m parameter before the illumination. The error bars indicate standard deviation from three biological replicates. Lines represent the best fit made to a first-order reaction.

3.3 Alternative methods to quantify photoinhibition and the calculation of the final k_{PI} values

The deviations from the first-order reaction kinetics with two free parameters in both organisms lead to an inspection of the results by plotting the data with four free parameters, according to equation $y = A_0 e^{-k_{PI_a} t} + B_0 e^{-k_{PI_b} t}$, where the overall rate constant of photoinhibition is the sum of two first-order reactions. In this equation, y reflects the overall activity of PSII complexes according to the used parameter at certain time point, A_0 reflects the overall activity of one PSII complex according to the used parameter before the photoinhibition, B_0 reflects the

overall activity of other PSII complex according to the used parameter before the photoinhibition, t is time, and finally k_{PIa} and k_{PIb} are the rate constants of photoinhibition. However, this led to results, where the error rates and P-values were too great for fit to predict the data reliably and better than first-order fits made with two free parameters. However, quantification using this method resulted in zero degree of freedom in the equation, as the fit involved four free parameters and only four data points. Therefore, the first-order fits made with four free parameters were ignored and not analyzed further. Besides the determination of the k_{PI} from first-order fits with using all data points and two free parameters, the rate constant was also calculated using only the first two data points by solving the k_{PI} from the equation $y = A_0 e^{-k_{PI} t}$. Determined through two first data points, calculated k_{PI} represents the initial reaction rate, which can be used to roughly illustrate the overall temperature dependency of the rate of photoinhibition in red and blue light.

After the plotting, the final k_{PI} values presented in the study are the result of the dark inactivation rate constant subtracted from the raw rate constant. Dark inactivation rate constants were determined from dark incubation treatments in the reaction system, whereas the raw rate constants were yielded from the high light photoinhibition treatments. Since the pumpkin thylakoids are isolated structures of a whole plant cell, decrease of the PSII activity in dark conditions was necessary to determine in order to see the effects of different temperatures by themselves. Similar analysis of photoinhibition was done to both *Synechocystis* to see the possible differences in temperature responses between the used strains. In *Synechocystis* however, dark incubation revealed no differences between two strains.

3.4 Temperature dependency of photoinhibition was found to be positive in pumpkin thylakoids in red and blue light and D_2O did not speed up photoinhibition

Calculated k_{PI} values were used to determine the temperature dependency of photoinhibition in red and blue light.

When k_{PI} values were calculated by using the first two data points, the temperature dependency of photoinhibition in pumpkin thylakoids was found to be positive in both light conditions, (Fig. 6). When photoinhibition treatments were quantified with the F_v/F_m parameter, the k_{PI} values approximately doubled in the used temperature range (Fig. 6B). Positive

temperature dependency was also found from the oxygen evolution results, but the increase of the k_{PI} was more subtle while moving towards higher temperatures (Fig. 6A).

When the k_{PI} values were determined from the first-order fits by using all data points and two free parameters, the temperature dependency of photoinhibition was also found to be positive in blue light (Fig. 7). The k_{PI} values approximately doubled in the used temperature range when the quantification was made with the F_v/F_m parameter (Fig. 7B). Increase of k_{PI} with the temperature was more subtle in blue light region, when the quantification was made with the oxygen evolution (Fig. 7A). In the red light region, photoinhibition was found to have a positive temperature dependency when quantified with the F_v/F_m parameter (Fig. 7B). However, the temperature dependency was lost when the quantification was done with oxygen evolution (Fig. 7A).

In addition to examining the temperature dependency of photoinhibition, D_2O was used to test the possible involvement of the $^1O_2$ in photoinhibition (Fig. 6, Fig. 7), by comparing k_{PI} values obtained from the D_2O treatments to corresponding treatments in water at the same temperatures and light color. D_2O prolongs the lifetime of $^1O_2$ compared to water surroundings (Khorobrykh et al., 2020). Based on the results by Mattila et al. (2023), the effect of $^1O_2$ is expected to be most pronounced while moving towards red light regions and higher temperatures.

When the quantification was based on the first two data points, photoinhibition was found to be slower in both red and blue light at 32 °C in D_2O-based medium compared to water-based medium (Fig. 6). k_{PI} values were also found to be lower in both red and blue light at 10 °C in D_2O-based medium compared to water-based medium when quantified with oxygen evolution (Fig. 6A). However, this was not the case when the quantification was made with the F_v/F_m parameter (Fig. 6B). In this case, k_{PI} was found to be greater in blue light and approximately the same as in red light in D_2O-based medium compared to water-based medium (Fig. 6B). Differences between D_2O- and water based treatments were found to be significant in red light at 32 °C ($P \leq 0.05$) (Fig. 6), when quantified with oxygen evolution and F_v/F_m parameter, and in blue light at 10 °C ($P \leq 0.01$) (Fig. 6B), when quantified with F_v/F_m parameter.

When the k_{PI} values were determined from the first-order fits by using all data points and two free parameters, photoinhibition was found to be slower in D_2O-based medium than in water-based medium in almost all conditions (Fig. 7). The only exception was in blue light at 10 °C, where photoinhibition was found to be greater in D_2O-based medium than in water-

based medium, when quantified with the F_v/F_m parameter (Fig. 7). Differences between k_{PI} in D_2O- and water-based treatments were found to be significant in both red and blue light at 10 °C ($P \leq 0.05$), and in red light at 32 °C ($P \leq 0.01$), when quantified with oxygen evolution (Fig. 7A). When quantified with the F_v/F_m parameter, differences between D_2O- and water-based treatments were found to be significant in blue light at 10 °C ($P \leq 0.01$), and in red light at 32 °C ($P \leq 0.01$) (Fig. 7B).

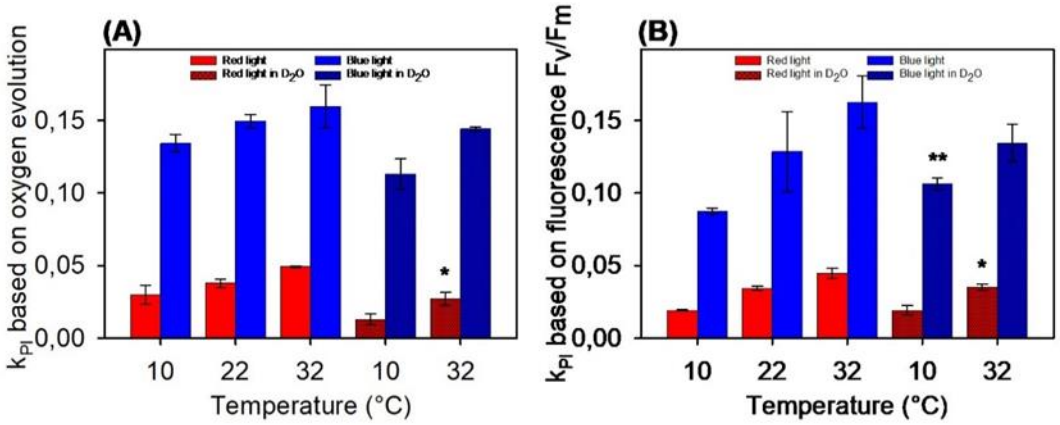

Figure 6. Temperature dependency of rate constant of photoinhibition (k_{PI}) in isolated pumpkin (*C. maxima*) thylakoids in red or blue light. k_{PI} was determined by using the first two data points of each experiment. Photoinhibition treatments were made either in water (light red and blue bars) or D_2O (dark red and blue bars). Quantification of photoinhibition was done with the light-saturated oxygen evolution rate of PSII in water with 0.5 mM 2,6-diclhorobenzoquinone (**A**), or with chlorophyll *a* fluorescence parameter F_v/F_m (**B**). Oxygen evolution rate of PSII was measured with Clark-type oxygen electrode in saturating white light at 22 °C. The F_v/F_m parameter was measured after 5 min of dark incubation at the room temperature. Quantification of photoinhibition was done at 0, 20, 40 and 60 min time points during the 60 min illumination, where the k_{PI} values were determined by using only the first two data points (0 and 20 min). PPFD in red light was 1000 µmol $m^{-2}s^{-1}$, whereas in blue light PPFD was 500 µmol $m^{-2}s^{-1}$. Results from the blue light treatments have been normalized to the PPFD of 1000 µmol $m^{-2}s^{-1}$ by multiplying the k_{PI} values with 2. The final k_{PI} values presented here were obtained by subtracting the dark inactivation rate constant from the raw rate constant derived directly from the photoinhibition treatments. Each k_{PI} value represents an averaged result from three biological replicates, and the error bars represent standard deviation. Statistical differences were analyzed with Student's *t* test (two-tailed; unequal variances), between k_{PI} values measured in water- and D_2O-based medium. Statistical differences are marked with *($P \leq 0.05$) and **($P \leq 0.01$) based on Student's *t* test.

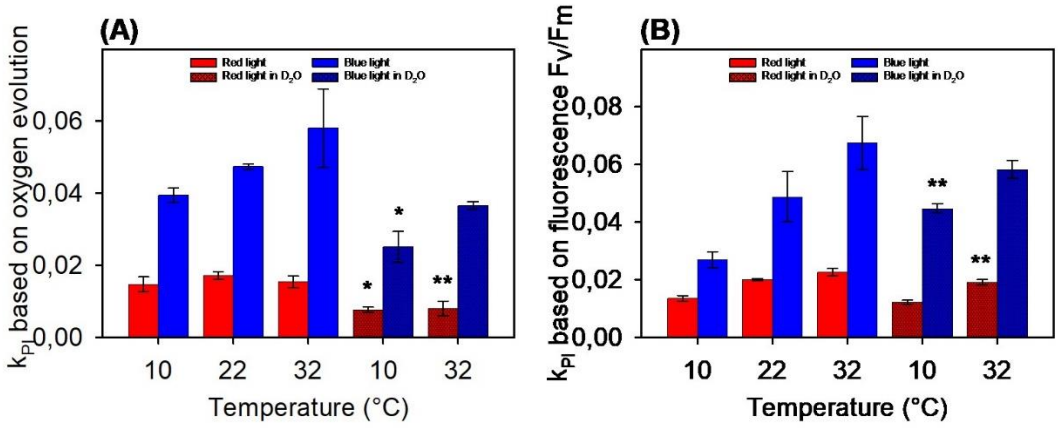

Figure 7. Temperature dependency of rate constant of photoinhibition (k_{PI}) in isolated pumpkin (*C. maxima*) thylakoids in red or blue light. k_{PI} was determined from the first-order fits of all data (4 data points). Photoinhibition treatments were made either in water (light red and blue bars) or D_2O (dark red and blue bars). Quantification of photoinhibition was done with the light-saturated oxygen evolution rate of PSII in water with 0.5 mM 2,6-diclhorobenzoquinone (**A**), or with chlorophyll *a* fluorescence parameter F_v/F_m (**B**). Oxygen evolution rate of PSII was measured with Clark-type oxygen electrode in saturating white light at 22 °C. The F_v/F_m parameter was measured after 5 min of dark incubation at the room temperature. Quantification of photoinhibition was done at 0, 20, 40 and 60 min time points during the 60 min illumination. PPFD in red light was 1000 µmol $m^{-2}s^{-1}$, whereas in blue light PPFD was 500 µmol $m^{-2}s^{-1}$. Results from blue light treatments have been normalized to the PPFD of 1000 µmol $m^{-2}s^{-1}$ by multiplying the k_{PI} values with 2. The final k_{PI} values presented here were obtained by subtracting the dark inactivation rate constant from the raw rate constant derived directly from the photoinhibition treatments. Each k_{PI} value represent an averaged result from three biological replicates, and the error bars represent standard deviation. Statistical differences were analyzed with Student's *t* test (two-tailed; unequal variances), between k_{PI} values measured in water- and D_2O-based medium. Statistical differences are marked with *($P \leq 0.05$) and **($P \leq 0.01$) based on Student's *t* test.

3.5 No temperature dependency of photoinhibition was found in either Synechocystis strains, whereas the ΔsigCDE showed some resistance against photoinhibition in red light

Similar analysis of photoinhibition under different condition was repeated for both *Synechocystis* strains. Similarly as done with pumpkin thylakoids, k_{PI} values were determined by fitting to two (Fig. 8) or four (Fig. 9) data points. The involvement of $^1O_2$ in photoinhibition was tested with the use of the ΔsigCDE mutant strain. Due to its high carotenoid contents (Pollari et al., 2011), ΔsigCDE strain is expected to show some resistance against photoinhibition when compared to CS. Once again, in the red light region at higher temperatures, the $^1O_2$ dependent pathway was expected to most clearly reveal the effects of $^1O_2$ in photoinhibition (Mattila et al. 2023).

When quantification was based on the first two data points, no temperature dependency in either light condition was found in either *Synechocystis* strain (Fig. 8). The result was the same

with both oxygen evolution and F_v/F_m parameter. When quantified with oxygen evolution, k_{PI} was found to be lower in the ΔsigCDE than in the CS in red light at 10, 32 and 40 °C (Fig. 8A). At 22 °C, k_{PI} was found to be approximately equal (Fig. 8A). In blue light, k_{PI} was found to be lower in the ΔsigCDE than in the CS at 10 and 22 °C, but greater in 32 and 40 °C (Fig. 8A). Statistically significant differences between the strains were found in red light at 10 °C ($P \leq 0.05$), and in blue light at 40 °C ($P \leq 0.05$) (Fig. 8A).

When the F_v/F_m parameter was used for the quantification, in red light k_{PI} values were found to be lower in the ΔsigCDE than in the CS at 32 °C, and approximately equal at 10, 22 and 40 °C (Fig. 8B). In blue light, the k_{PI} values were found to be lower in the ΔsigCDE than in the CS at 22 °C, and greater at all other temperatures (Fig. 8B). With the F_v/F_m parameter, statistically significant differences between the strains were found in the blue light at 22 and 40 °C ($P \leq 0.01$) (Fig. 8B).

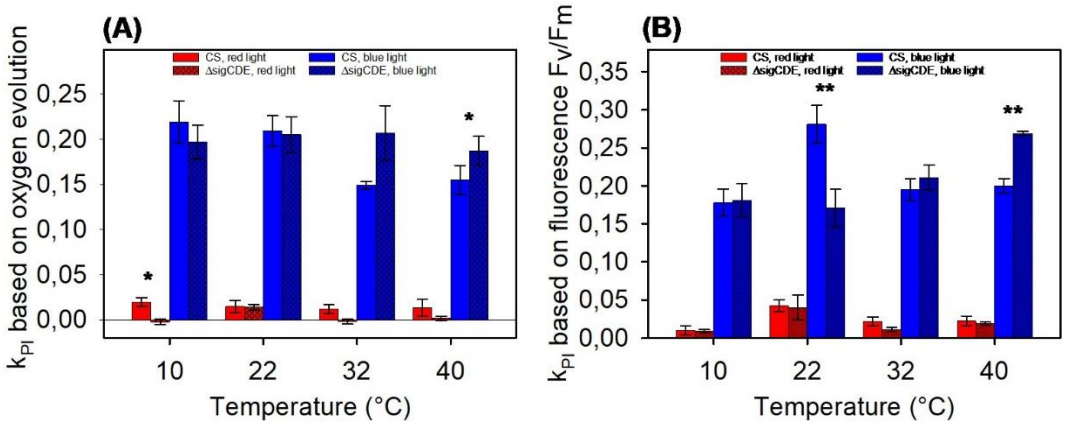

Figure 8. Temperature dependency of rate constant of photoinhibition (k_{PI}) in *Synechocystis* sp. PCC 6803 GT-T (CS) (light red and blue bars), and in *Synechocystis* sp. PCC 6803 ΔsigCDE (dark red and blue bars) in red or blue light. k_{PI} was determined by using first the first two data points of each experiment. Quantification of the photoinhibition was done with the light-saturated oxygen evolution rate of PSII in water with 0.5 mM 2,6-diclhorobenzoquinone and 0.5 mM ferricyanide (**A**), or with chlorophyll *a* fluorescence parameter F_v/F_m (**B**). Oxygen evolution rate of PSII was measured with Clark-type oxygen electrode in saturating white light at 32 °C. The F_v/F_m parameter was measured after 5 min of dark incubation at room temperature. Quantification of photoinhibition was made at 0, 30, 60 and 90 min time points, or at 0, 20, 40 and 60 min time points, during the 90 or 60 min illumination, where the k_{PI} values were determined by using only first two data points (0 and 30 min or 0 and 20 min). Lincomycin was used right before the treatments. PPFD in red light was 1000 µmol $m^{-2}s^{-1}$, whereas in blue light PPFD was 350 µmol $m^{-2}s^{-1}$. Results from blue light treatments have been normalized to the PPFD of 1000 µmol $m^{-2}s^{-1}$ by multiplying the k_{PI} values with 2.85. The final k_{PI} values presented here were obtained by subtracting the dark inactivation rate constant from the raw rate constant derived directly from the photoinhibition treatments. Each k_{PI} value represent an averaged result from three biological replicates, whereas the error bars represent standard deviation. Statistical differences were analyzed with Student's *t* test (two-tailed; unequal variances), between k_{PI} values measured with the CS and ΔsigCDE in certain light condition, and at certain temperature. Statistically significant differences are marked with *(P≤0.05) and **(P≤0.01) based on Student's *t* test.

When the k_{PI} values were determined from the first-order fits by using all data points and two free parameters, quantification with oxygen evolution showed the temperature dependency of photoinhibition to be negative in the blue light in both strains (Fig. 9A). In red light, no temperature dependency was found (Fig. 9A). The k_{PI} values were lower in the ΔsigCDE than in the CS in red light at 10, 32 and 40 °C, whereas the k_{PI} was found to be approximately equal at 22 °C (Fig. 9A). In blue light, the k_{PI} values were found to be greater in the ΔsigCDE than in the CS at all temperatures (Fig. 9A). Statistically significant differences between the strains were found in red light at 40 °C (P≤0.01), and in blue light at 10 °C (P≤0.01) (Fig. 9A).

On the contrary, quantification with the F_v/F_m parameter showed the temperature dependency of photoinhibition to be positive in the ΔsigCDE strain in blue light, whereas no temperature

dependency for the CS was found (Fig. 9B). In red light, no temperature dependency was found for either strain (Fig. 9B). Between the strains, the k_{PI} values were found to be lower in the ΔsigCDE than in the CS in red light at all temperatures (Fig. 9B). In blue light, the k_{PI} values were found to be lower in the ΔsigCDE than in the CS at 10 and 22 °C, and greater at 32 and 40 °C (Fig. 9B). Statistically significant differences between the strains were found in the blue light at 22 (P≤0.05) and 40 °C (P≤0.01) (Fig. 9B).

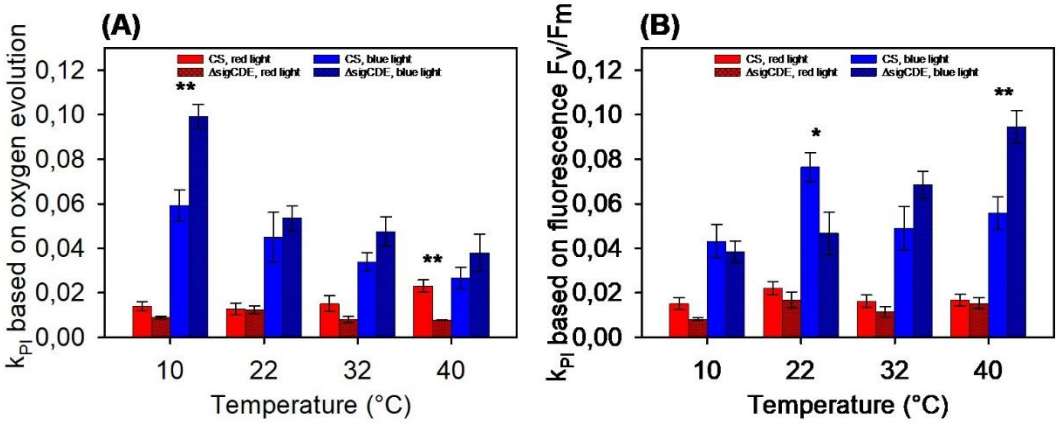

Figure 9. Temperature dependency of rate constant of photoinhibition (k_{PI}) in *Synechocystis* sp. PCC 6803 GT-T (CS) (light red and blue bars), and in *Synechocystis* sp. PCC 6803 ΔsigCDE (dark red and blue bars), in red or blue light. k_{PI} was determined from the first-order fits of all data (4 data points). Quantification of the photoinhibition was done with the light-saturated oxygen evolution rate of PSII in water with 0.5 mM 2,6-diclhorobenzoquinone and 0.5 mM ferricyanide (**A**), or with chlorophyll *a* fluorescence parameter F_v/F_m (**B**). Oxygen evolution rate of PSII was measured with Clark-type oxygen electrode in saturating white light at 32 °C. The F_v/F_m parameter was measured after 5 min of dark incubation at room temperature. Quantification of photoinhibition was made at 0, 30, 60 and 90 min time points, or at 0, 20, 40 and 60 min time points, during the 90 or 60 min illumination. Lincomycin was used right before the treatments. PPFD in red light was 1000 µmol $m^{-2}s^{-1}$, whereas in blue light PPFD was 350 µmol $m^{-2}s^{-1}$. Results from blue light treatments have been normalized to the PPFD of 1000 µmol $m^{-2}s^{-1}$ by multiplying the k_{PI} values with 2.85. The final k_{PI} values presented here were obtained by subtracting the dark inactivation rate constant from the raw rate constant derived directly from the photoinhibition treatments. Each k_{PI} value represent an averaged result from three biological replicates, whereas the error bars represent standard deviation. Statistical differences were analyzed with Student's *t* test (two-tailed; unequal variances), between k_{PI} values measured with the CS and ΔsigCDE in certain light condition, and at certain temperature. Statistically significant differences are marked with *(P≤0.05) and **(P≤0.01) based on Student's *t* test.

4 Discussion

4.1 Deviation from first-order kinetics

Photoinhibition is consistently shown to follow the first-order reaction kinetics (see for example (Sarvikas et al., 2010; Tyystjärvi, 2013). That is to say, active PSII centers act as an only substrate of photoinhibition, which leads to repeatedly observed first-order behavior. Results have been consistent regardless the method used in the quantification of photoinhibition (Tyystjärvi, 2013). Still in this study, a deviation from first-order kinetics was observed in almost all experiments, regardless of the used conditions (Figs. 2, 3, 4, 5). In addition, deviations were found to occur in both organisms, also both *in vitro* and *in vivo* (Figs. 2, 3, 4, 5). In all cases, the deviation from first-order kinetics was most evident in the fits made out of individual experiments. Therefore, scattering of the averaged data doesn't explain the observed results. What is more, the deviation from the first-order kinetics was more evident in the quantification made through oxygen evolution (Figs. 2AB, 3AB, 4AB, 5AB), even though the deviation could be observed in both *Synechocystis* strains when the quantification was made with F_v/F_m parameter (Figs. 4CD, 5CD).

Regardless of the prevailing consensus on the first-order kinetics of photoinhibition, opposing results about the first-order kinetics have been obtained (Lee et al., 2001; Matsubara & Chow, 2004; Sun et al., 2006). In these studies, photoinhibition was found to deviate from the first-order kinetics after prolonged illumination (Lee et al., 2001; Matsubara & Chow, 2004). These findings led to a suggestion that in prolonged photoinhibition photodamaged and inactivated PSII reaction centers protect the remaining active ones (Sun et al., 2006). However, similar kinds of results were not obtained in the further study by Sarvikas et al. (2010), where prolonged photoinhibition was found to follow the first-order kinetics, without photodamaged PSII centers giving any additional protection. The difference between the studies remains unsolved.

Comparing the obtained results to above-mentioned studies, couple of differences remain. First of all, it should be underlined that previous studies in question have observed, or studied, the deviation from the first-order kinetics only after the prolonged photoinhibition. Here however, the deviation from the first-order kinetics was observed after relatively short illumination time (Figs. 2, 3, 4, 5). After the short illumination, the decrease of the PSII activity was found to be too steep compared to first-order fits (Figs. 2, 3, 4, 5). In other words, either the loss of oxygen evolution ability or the decrease of F_v/F_m was found to be too rapid due to light-induced damage.

However, it should be noted that the recent findings about the kinetics of PSII reaction centers call for a careful re-evaluation of how the F_v/F_m parameter reflects the quantum yield of Chl *a* fluorescence (Sipka et al., 2021).

Possible explanation may lay in the different mechanisms of photoinhibition, where the damage targets the different sites of PSII. This theory should fit into the context of conducted study, where different light conditions were used to differentiate the mechanisms of photoinhibition. In the used blue light region, manganese mechanism is expected to be the prevailing mechanism of photoinhibition, whereas in the red light region $^1O_2$ or P_{680}^+ dependent pathways should be more prominent (Mattila et al., 2023). However, similar kinds of results of the deviation from first-order kinetics was obtained in all conditions, and especially in both light circumstances, disproving the explanation of the deviation from first-order kinetics due to different mechanisms and sites of damage in photoinhibition (Figs. 2, 3, 4, 5).

The second interesting curiosity in the obtained results was the role of lincomycin. In the previous studies, lincomycin was used in all cases, when the deviation from the first-order kinetics was observed (Lee et al., 2001; Matsubara & Chow, 2004; Sun et al., 2006). In this study, lincomycin was used only with both cyanobacteria, but not with isolated pumpkin thylakoids, where the deviations from the first-order kinetics were the most evident (Figs. 2, 3, 4, 5). In other words, deviation from the first-order kinetics was most evident when the PSII repair cycle and the synthesis of the D1 protein were not existent. This suggests that the uptake of lincomycin and the dynamic response to photoinhibition could not be used to explain the result. The obtained results point toward intrinsic properties of PSII in isolated pumpkin thylakoids as a likely explanation for the deviation from the first-order kinetics. In addition, the results yielded from isolated pumpkin thylakoids are also contrary to the study by Sarvikas et al. (2010), where the photoinhibition of isolated pumpkin thylakoids clearly followed first-order kinetics. However, the role of the lincomycin cannot be fully ruled out without further investigation.

In conclusion, more research about the deviation from first-order kinetics in the context of this study is needed. More careful analysis of the data would be required, in addition to more repetitions of the study. For example, higher lincomycin concentration and its functionality at all temperatures should be examined. Additionally, better fits were not obtained through the different fits of the data, which also underlines the need for further investigation of the phenomenon obtained in the context of this study.

4.2 Temperature dependency of photoinhibition

The studies in temperature dependency of photoinhibition has yielded varying results in the literature. Temperature dependency of photoinhibition has found to be positive in multiple studies (see for example Tyystjärvi et al., 1994; Ueno et al., 2016; Mattila et al., 2020; Mattila et al., 2023), whereas also negative correlation has been obtained (Kornyeyev et al., 2003; Tsonev & Hikosaka, 2003). The results are obtained from both in vivo and in vitro experiments, with different kinds of model organisms. Additionally, in some cases no changes in the rate constant of photoinhibition at different temperatures has been found (Allakhverdiev & Murata, 2004). Results in the present study tilt to all of these previous findings (Figs. 6, 7, 8, 9).

In isolated pumpkin thylakoids, positive temperature dependency, or no temperature dependency at all was found to photoinhibition (Figs. 6, 7). Results with the positive temperature dependency of photoinhibition *in vitro* are in accordance with several studies, where both quantification methods are used in the determination of k_{PI} (Tyystjärvi et al., 1994; Mattila et al., 2023, 2020). No temperature dependency at all was found only in red light, when the quantification of the photoinhibition was made with oxygen evolution through first-order fits with all data points (Fig. 7A). In this case, rate constant of the photoinhibition remained approximately the same throughout the whole temperature range (Fig. 7A). Differences in the results of Tsonev and Hikosaka (2003) and Kornyeyev et al. (2003) could be explained with the use of the F_v/F_m parameter. Besides the cold treatments, the parameter was also measured at low temperatures in the studies in question. Tsonev and Hikosaka (2003) also made the dark incubation at low temperatures. In these cases, the decrease of the F_v/F_m parameter might reflect the fluorescence quenching induced in low temperatures, which might not relax in the typical dark-adaptation time at low temperature. This results in the decrease of F_v/F_m parameter, and false decrease of the PSII activity regarding photoinhibition. In addition, finding of the negative temperature dependency of photoinhibition was made *in vivo*, not *in vitro*, so the results cannot be directly compared (Kornyeyev et al., 2003; Tsonev & Hikosaka, 2003).

On the contrary, the temperature dependency of photoinhibition in both Synechocystis strains yielded results that are not in accordance with earlier studies (Ueno et al., 2016; Mattila et al., 2023). Even though negative or positive temperature dependency could be found in either *Synechocystis* strain depending on the quantification method, no conclusion of the temperature dependency of photoinhibition could be made (Figs. 8, 9). For example, temperature dependency was found to be opposite in the CS, when the quantification was done in different

method (Fig. 9). In addition, when no temperature dependency was found in either *Synechocystis* strains, the results were scattered all over in both light conditions and at different temperatures (Figs. 8, 9). This confirms the interpretation of the results that no temperature dependency was found in either *Synechocystis* strains.

Explanation to observed results with *Synechocystis* might lay in the used light conditions, which were made by the using different filters. In the red light region, the chosen filter transmitted light above 600 nm, whereas in the blue light filter transmitted light below 450 nm (Fig. 1). In addition, UV-filter in the used system blocked the UV-radiation below 400 nm (Fig. 1). Especially the usage of the selected red light filter should be taken into closer inspection, as the results showed more scattering and inconsistency compared to blue light (Figs. 8, 9). In cyanobacteria, the light harvesting antenna is composed of bilin pigment molecules, which together with covalently bound proteins form a phycobilisome responsible of light harvesting in the outer PSII antenna. Phycobilisomes have a vast absorption spectrum in the range between 450 and 650 nm, making them efficient light harvesting complexes in cyanobacteria (Mullineaux, 2008; X. Li et al., 2023). In *Synechocystis*, the absorption spectrum of phycobilisomes is approximately between 570 and 650 nm (Lea-Smith et al., 2014). In the context of PSII, the light absorption of phycobilisomes is important above 600 nm, when moving towards the red light region. However, in this study the use of light at 600 nm and above might have affected the obtained result, where the light absorption might have been made by another pigment molecule complex besides the phycobilisome. Therefore, using a long-pass filter with a cutoff above 600 nm (e.g., 610 or 620 nm) might have provided greater specificity for phycobilisomes and PSII, potentially leading to different results.

One possible pigment molecule complex responsible for the obtained result might have been OCP. In cyanobacteria, OCPs are responsible for the dissipation of the excess light energy via NPQ (Kerfeld, 2017). In high-light conditions, light absorbance by OCP results in an active form of the protein that binds to phycobilisome and quenches the excessive excitation energy (Niyogi & Truong, 2013). This activated NPQ by OCP could affect the temperature dependency of photoinhibition, especially at the higher temperatures, where the NPQ is activated more efficiently. In other words, NPQ prevents the light-induced damage of photoinhibition at higher temperatures, resulting in the obtained result in red light region (Figs. 8, 9). However, the NPQ and OCP are mainly activated in the blue-green light region in *Synechocystis* (Kirilovsky & Kerfeld, 2012), leaving the obtained result in red light open for question.

As for blue light, NPQ and OCP is suggested to play larger role in quenching the excessive excitation energy. According to this theory, NPQ should give protection against light-induced damage of photoinhibition at higher temperatures. This supported by the results shown in Fig. 9A, where the temperature dependency of photoinhibition is negative in both *Synechocystis* strains. However, the inconsistency of the temperature dependency of photoinhibition in all other blue light results also leaves obtained results open for question (Fig. 8, Fig. 9B). In addition, it should be also noted that NPQ is suggested to not give protection against the prevailing manganese mechanism of photoinhibition in blue light region (Tyystjärvi 2013).

The other factor affecting the obtained result in *Synechocystis* might have been the use of lincomycin and its proper functions. Even though there were no indications of lincomycin not working like it was supposed to, the effects of using lincomycin should be tested in the experimental setup to rule out this possibility.

4.3 The involvement of $^1O_2$ in photoinhibition in the red light region

The involvement of $^1O_2$ in photoinhibition of PSII has been suggested by several studies (for review, see Vass, 2012; Tyystjärvi, 2013). It is proposed that $^1O_2$ itself acts as a damaging agent in photoinhibition, causing the irreversible light-induced damage of PSII (Vass, 2012). However, several other facts point out that the $^1O_2$ dependent mechanism could not be the only pathway for photoinhibition under visible light (Hakala et al., 2005; Tyystjärvi, 2013) Other mechanisms associate the manganese ions of OEC or the P_{680}^+ to be responsible of photoinhibition in PSII. Exact molecular mechanism or mechanisms of photoinhibition under visible light remain under debate. Recent study by Mattila et al. (2023) suggested that photoinhibition has three parallel mechanisms in the range of visible light, where all aforementioned mechanisms are involved. The results of the same study also suggest that the $^1O_2$ dependent pathway should be enhanced in the red light region.

In this study, the possible involvement of the $^1O_2$ was monitored through D_2O-based medium and *Synechocystis* sp. PCC 6803 ΔsigCDE. In D_2O, the lifetime of $^1O_2$ is prolonged by many folds, enabling it to act as a damaging agent more freely. In the water-based medium, the $^1O_2$ loses its energy commonly through dissipation by interacting with water molecules. On the other hand, the ΔsigCDE strain was used for its high carotenoid contents inside of the cell.

Carotenoids act as an important antioxidant against $^1O_2$, which were expected to give the ΔsigCDE mutant resistance against $^1O_2$ in photoinhibition.

4.3.1 The prolonged lifetime of $^1O_2$ in D_2O does not speed up the photoinhibition

Photoinhibition treatments made in D_2O were not found to proceed any faster when compared to water-based medium (Figs. 6, 7). In almost all cases, k_{PI} values from the D_2O treatments are lower compared to water-based medium (Figs. 6, 7). However, two exceptions can be found in red and blue light at 10 °C when quantification was made with the F_v/F_m parameter (Figs. 6B, 7B). In this case, k_{PI} values of D_2O treatments were found to be greater in blue light at 10 °C compared to corresponding treatments made in water (Figs. 6B, 7B). This outcome was consistent regardless of whether the k_{PI} was determined by using the first two or all data points. However, when the quantification was made with the oxygen evolution, photoinhibition treatments in D_2O was found to proceed more slowly in both light conditions and at both temperatures compared to treatments in water-based medium (Figs. 6A, 7A), making the F_v/F_m result open to question.

Not that of many studies about photoinhibition in D_2O-based medium exist. Result obtained here are in line with the study by Sopory et al. (1990), where photoinhibition was also found to be slower in the D_2O surroundings. However, the results were obtained from *in vivo* experiments in the study in question, so the results cannot be compared directly. In other study by Jung & Kim (1990), photoinhibition was found to be faster in the D_2O-based medium *in vitro*. These results are opposite to those yielded in this study.

Results of photoinhibition in D_2O-based medium speak against the involvement of $^1O_2$ in photoinhibition. However, other possibilities of the involvement of $^1O_2$ still remain open. It is also possible that $^1O_2$ causes damage before it enters the soluble phase. That is to say, $^1O_2$ reacts in the near vicinity of its evolving site with the surrounding proteins, lipids and pigment molecules. In that case, the effects of the solvent prolonging the lifetime of $^1O_2$ doesn't matter. $^1O_2$ is also known to inhibit the PSII repair cycle (Nishiyama et al., 2004). The results obtained here suit to this observation, where the effects of $^1O_2$ are indirect to photoinhibition. However, it should be noted that in this study the D_2O-based medium was used only with isolated pumpkin thylakoids where the PSII repair cycle is nonexistent. Therefore, further investigation with fully functional PSII repair cycle and the effects of $^1O_2$ would be needed.

4.3.2 ΔsigCDE strain showed resistance against photoinhibition in red light

Compared to CS, the ΔsigCDE strain showed resistance against photoinhibition in the red light region (Figs. 8, 9). However, the results showed only a trend of resistance against photoinhibition, where statistical differences between the strains were only found at 10 and 40 °C (Figs. 8A, 9A). In these cases, the quantification was made with oxygen evolution, and k_{PI} was determined either by using first-order fits made with the first two (Fig. 8A) or all (Fig. 9A) data points. In any case, results in the red light showed more consistency compared to blue light (Figs. 8, 9). Also, a word about the determination method of k_{PI} by the first two data points should be mentioned in the case of *Synechocystis*. With both *Synechocystis* strains, the illumination in the red light was prolonged to 90 min in order to see the possible differences in the strains after longer treatment time. However, the effects of prolonged illumination are not evident in the k_{PI} values determined through the first two data points. This could explain the differences of the results in the red light with *Synechocystis*, where the difference between the strains is not that evident in the k_{PI} values determined by first two data point compared to k_{PI} yielded from multiple data points (Figs. 8, 9).

In blue light region, the situation was quite different with the ΔsigCDE strain (Figs. 8, 9). Compared to CS, the ΔsigCDE showed to be more sensitive to photoinhibition at almost all temperatures. Here again however, the results show some variance between the quantification methods and the way k_{PI} was determined, so clear conclusions cannot be made (Figs. 8, 9).

Results obtained from here are partly in accordance with the study by Hakkila et al. (2014), where the ΔsigCDE strain was found to be more resistant against photoinhibition. Similar kinds of results were obtained in red light, whereas the results from blue light were different (Figs. 8, 9). In the study by Hakkila et al. (2014), the illumination of the *Synechocystis* strains were made in saturating white light, so the results cannot be compared directly. However, the observed result fits to a hypothesis of photoinhibition, in which photoinhibition is caused by $^1O_2$ especially in the red light region (Mattila et al., 2023). Due to its high carotenoid contents, ΔsigCDE strain is expected to be more resistant against the damages of $^1O_2$ compared to CS. In the case of this study, ΔsigCDE strain should be more resistant to photoinhibition if $^1O_2$ is involved in the damaging reactions. Results obtained here show slight indications of this in red light (Figs. 8, 9), even though more research is obviously needed. For example, other detection methods of the involvement of $^1O_2$ in the red light region would be necessary. Interestingly in

the same study by Hakkila et al. (2014), ΔsigCDE strain showed to be more sensitive against oxidative stress in standard conditions. Also this in mind, it would be necessary to specify the involvement of the $^1O_2$ under different conditions.

4.4 Conclusions

To conclude, the aim of the thesis was to investigate the possible involvement of $^1O_2$ in photoinhibition under different temperature and light conditions. Firstly, the temperature dependency of photoinhibition was found to vary between the *in vitro* experiments with pumpkin, and *in vivo* experiments with cyanobacteria. In isolated pumpkin thylakoids, the temperature dependency of photoinhibition was found to be positive in both light conditions, whereas in *Synechocystis* no temperature dependency was found in either strain. Secondly, in isolated pumpkin thylakoids photoinhibition treatments in D_2O proceeded more slowly compared to water-based medium, suggesting that the effect of $^1O_2$ lifetime in the solvent is small in photoinhibition. However, ΔsigCDE strain was found to be more resistant against photoinhibition compared to CS in red light region, suggesting the possible involvement of $^1O_2$ in photoinhibition. Lastly, an interesting deviation from the expected first-order kinetics in photoinhibition was observed in both *in vitro* and *in vivo* experiments. Deviations were most evident in *in vitro* treatments with pumpkin thylakoids after relatively short light exposure.

References

Allakhverdiev, S. I., & Murata, N. (2004). Environmental stress inhibits the synthesis de novo of proteins involved in the photodamage-repair cycle of Photosystem II in *Synechocystis* sp. PCC 6803. Biochimica et Biophysica Acta - Bioenergetics 1657, 23–32. https://doi.org/ 10.1016/j.bbabio.2004.03.003

Allen, J. F. (2003). Cyclic, pseudocyclic and noncyclic photophosphorylation: new links in the chain. Trends in Plant Science 8, 15–19. https://doi.org/10.1016/S1360-1385(02)00006-7

Anderson, J. M., Park, Y.-I., Chow, W. S. (1998). Unifying model for the photoinactivation of Photosystem II in vivo under steady-state photosynthesis. Photosynthesis Research 56, 1–13. https://doi.org/10.1023/A:1005946808488

Andersson, B., & Anderson, J. M. (1980). Lateral heterogenity in the distribution of chlorophyll-protein complexes of the thylakoid membranes of spinach chloroplasts. Biochimica et Biophysica Acta – Bioenergetics 593, 427–40. https://doi.org/10.1016/ 0005-2728(80)90078-x

Aro, E. M., Suorsa, M., Rokka, A., Allahverdiyeva, Y., Paakkarinen, V., Saleem, A., Battchikova, N., & Rintamäki, E. (2005). Dynamics of photosystem II: A proteomic approach to thylakoid protein complexes. Journal of Experimental Botany 56, 347–356. https://doi.org/10.1093/jxb/eri041

Berera, R., Van Stokkum, I. H. M., Gwizdala, M., Wilson, A., Kirilovsky, D., & Van Grondelle, R. (2012). The photophysics of the orange carotenoid protein, a light-powered molecular switch. Journal of Physical Chemistry B 116, 2568–2574. https://doi.org/ 10.1021/jp2108329

Berry, J. O., Yerramsetty, P., Zielinski, A. M., & Mure, C. M. (2013). Photosynthetic gene expression in higher plants. Photosynthesis Research 117, 91–120. https://doi.org/10.1007/s11120-013-9880-8

Bhatti, A. F., Choubeh, R. R., Kirilovsky, D., Wientjes, E., & van Amerongen, H. (2020). State transitions in cyanobacteria studied with picosecond fluorescence at room temperature. Biochimica et Biophysica Acta - Bioenergetics 1861, 148255. https://doi.org/10.1016 /j.bbabio.2020.148255

Bonardi, V., Pesaresi, P., Becker, T., Schleiff, E., Wagner, R., Pfannschmidt, T., Jahns, P., & Leister, D. (2005). Photosystem II core phosphorylation and photosynthetic acclimation require two different protein kinases. Nature 437, 1179–1182. https://doi.org/ 10.1038/nature04016

Cardona, T., Sánchez-Baracaldo, P., Rutherford, A. W., & Larkum, A. W. (2019). Early Archean origin of Photosystem II. Geobiology 17, 127–150. https://doi.org/ 10.1111/gbi.12322

Cazzaniga, S., Li, Z., Niyogi, K. K., Bassi, R., & Dall'Osto, L. (2012). The Arabidopsis szl1 mutant reveals a critical role of β-carotene in photosystem I photoprotection. Plant Physiology 159, 1745–1758. https://doi.org/10.1104/pp.112.201137

De Wijn, R., & Van Gorkom, H. J. (2001). Kinetics of electron transfer from Q_A to Q_B in photosystem II. Biochemistry 40, 11912–11922. https://doi.org/10.1021/bi010852r

Di Mascio, P., Martinez, G. R., Miyamoto, S., Ronsein, G. E., Medeiros, M. H. G., & Cadet, J. (2019). Singlet molecular oxygen reactions with nucleic acids, lipids, and proteins. Chemical reviews 119, 2043–2086. https://doi.org/10.1021/acs.chemrev.8b00554

Diner, B. A., Schlodder, E., Nixon, P. J., Coleman, W. J., Rappaport, F., Lavergne, J., Vermaas, W. F. J., & Chisholm, D. A. (2001). Site-directed mutations at D1-His198 and D2-His197 of photosystem II in *Synechocystis* PCC 6803: Sites of primary charge separation and cation and triplet stabilization. Biochemistry 40, 9265–9281. https://doi.org/ 10.1021/bi010121r

El Bissati, K., Delphin, E., Murata, N., Etienne, A.-L., & Kirilovsky, D. (2000). Photosystem II fluorescence quenching in the cyanobacterium *Synechocystis* PCC 6803: involvement of two different mechanisms. Biochemica et Biophysica Acta - Bioenergetics 1457, 229-42. https://doi.org/ 10.1016/s0005-2728(00)00104-3.

Fischer, W. W., Hemp, J., & Johnson, J. E. (2016). Evolution of oxygenic photosynthesis. Annual Review of Earth and Planetary Sciences 44, 647–683. https://doi.org/10.1146/ annurev-earth-060313-054810

Foyer, C.H.; Trebst, A.; Noctor, G. (2008) Signaling and integration of defense functions of tocopherol, ascorbate and glutathione. In *Photoprotection, Photoinhibition, Gene Regulation, and Environment. Advances in Photosynthesis and Respiration* (Demmig-Adams, B., Adams,W.W., Mattoo, A.K., Eds.), pp. 241–268. Springer, Dordrecht, The Netherlands

Groot, M.L., Pawlowicz N.P., van Wilderen, L.J.G.W., Breton, J., van Stokkum, I.H.M., van Grondelle, R. (2005) Initial electron donor and acceptor in isolated photosystem II reaction centers identified with femtosecond mid-IR spectroscopy. Proceedings of the National Academy of Sciences of the United States of America 102, 13087-13092. https://doi.org/10.1073/pnas.0503483102

Hakala, M., Tuominen, I., Keränen, M., Tyystjärvi, T., & Tyystjärvi, E. (2005). Evidence for the role of the oxygen-evolving manganese complex in photoinhibition of Photosystem II. Biochimica et Biophysica Acta - Bioenergetics 1706, 68–80. https://doi.org/10.1016 /j.bbabio.2004.09.001

Hakkila, K., Antal, T., Gunnelius, L., Kurkela, J., Matthijs, H. C. P., Tyystjärvi, E., & Tyystjarvi, T. (2013). Group 2 sigma factor mutant ΔsigCDE of the cyanobacterium *Synechocystis* sp. PCC 6803 reveals functionality of both carotenoids and flavodiiron proteins in photoprotection of photosystem II. Plant & Cell Physiology 54, 1780–1790. https://doi.org/10.1093/pcp/pct123

Hakkila, K., Antal, T., Rehman, A. U., Kurkela, J., Wada, H., Vass, I., Tyystjärvi, E., & Tyystjärvi, T. (2014). Oxidative stress and photoinhibition can be separated in the cyanobacterium *Synechocystis* sp. PCC 6803. Biochimica et Biophysica Acta - Bioenergetics, 1837, 217–225. https://doi.org/10.1016/j.bbabio.2013.11.011

Havurinne, V., Mattila H., Antinluoma, M., Tyystjärvi, E. (2019) Unresolved quenching mechanisms of chlorophyll fluorescence may invalidate MT saturating pulse analyses of photosynthetic electron transfer in microalgae. Physiolgica Plantarum 166, 365–379. https://doi.org/10.1111/ppl.12829

Hideg, É., Kós, P. B., & Vass, I. (2007). Photosystem II damage induced by chemically generated singlet oxygen in tobacco leaves. Physiologica Plantarum 131, 33–40. https://doi.org/10.1111/j.1399-3054.2007.00913.x

Jegerschlöd, C., Virgin, I., & Styring, S. (1990). Light-dependent degradation of the D1 protein in photosystem II is accelerated after inhibition of the water splitting reaction. Biochemistry 29, 6179-86. https://doi.org/10.1021/bi00478a010

Jimbo, H., Noda, A., Hayashi, H., Nagano, T., Yumoto, I., Orikasa, Y., Okuyama, H., & Nishiyama, Y. (2013). Expression of a highly active catalase VktA in the cyanobacterium *Synechococcus elongatus* PCC 7942 alleviates the photoinhibition of photosystem II. Photosynthetic Research 117, 509–515. https://doi.org/10.1007/s11120-013-9804-7

Jones, L. W., & Kok, B. (1966). Photoinhibition of chloroplast reactions. I. Kinetics and Action Spectra. Plant Physiology. 41, 1037-43. https//:doi.org10.1104/pp.41.6.1037.

Jung, J., Kim, H.-S. (1990). The chromophores as endogenous sensitizers involved in the photogeneration of singlet oxygen in spinach thylakoids. Photochemstry and Photobiology. 52, 1003–1009. https://doi.org/10.1111/j.1751-1097.1990.tb01817.x

Järvi, S., Suorsa, M., & Aro, E. M. (2015). Photosystem II repair in plant chloroplasts - regulation, assisting proteins and shared components with photosystem II biogenesis. Biochimica et Biophysica Acta - Bioenergetics 1847. 900–909). https://doi.org/10.1016/ j.bbabio.2015.01.006

Kawakami, K., Umena, Y., Kamiya, N., & Shen, J.-R. (2009). Location of chloride and its possible functions in oxygen-evolving photosystem II revealed by X-ray crystallography. Proceedings of the National Academy of Sciences of the United States of America 106, 8567-8572. https://doi.org/10.1073/pnas.0812797106

Keeling, P. J. (2004). Diversity and evolutionary history of plastids and their hosts. American Journal of Botany 91, 1481–1493. https://doi.org/10.3732/ajb.91.10.1481

Keren, N., Berg, A., Van Kan, P. J. M., Levanon, H., & Ohad, I. (1997). Mechanism of photosystem II photoinactivation and D1 protein degradation at low light: The role of back electron flow. Proceedings of the National Academy of Sciences of the United States of America 94,1579-84. https://doi.org 10.1073/pnas.94.4.1579.

Kerfeld, C. A., Melnicki, M. R., Sutter, M., & Dominguez-Martin, M. A. (2017). Structure, function and evolution of the cyanobacterial orange carotenoid protein and its homologs. New Phytologist 215, 937–951. https://doi.org/10.1111/nph.14670

Khorobrykh, S., Havurinne, V., Mattila, H., & Tyystjärvi, E. (2020). Oxygen and ROS in photosynthesis. Plants 9, 91. https://doi.org/10.3390/plants9010091

Kirilovsky, D., Kerfeld, C. A. (2012). The orange carotenoid protein in photoprotection of photosystem II in cyanobacteria. Biochimica et Biophysica Acta - Bioenergetics 1817, 158–166. https://doi.org/10.1016/j.bbabio.2011.04.013

Klauss, A., Haumann, M., & Dau, H. (2012). Alternating electron and proton transfer steps in photosynthetic water oxidation. Proceedings of the National Academy of Sciences of the United States of America 109, 16035-40. https://doi.org/10.1073/pnas.1206266109

Kok B, Forbush B, McGloin M (1970) Cooperation of charges in photosynthetic O2 evolution. I. A linear four step mechanism. Photochemistry and Photobiology. 11, 457–475. https://doi.org/10.1111 /j.1751-1097.1970.tb06017.

Kornyeyev, D., Holaday, S., & Logan, B. (2003). Predicting the extent of photosystem II photoinactivation using chlorophyll *a* fluorescence parameters measured during illumination. Plant & Cell Physiology 44, 1064-1070. https://doi.org/10.1093/pcp/pcg129

Krasnovsky, A. A. (1994). Singlet molecular oxygen and primary mechanisms of photo-oxidative damage of chloroplasts. Studies based on detection of oxygen and pigment phosphorescence. Proceedings of the Royal Society of Edinburgh. Section B. Biological Sciences 102, 219–235. https://doi.org/10.1017/s0269727000014147

Krieger-Liszkay, A. (2005). Singlet oxygen production in photosynthesis. Journal of Experimental Botany 56, 337–346. https://doi.org/10.1093/jxb/erh237

Krieger-Liszkay, A., & Trebst, A. (2006). Tocopherol is the scavenger of singlet oxygen produced by the triplet states of chlorophyll in the PSII reaction centre. Journal of Experimental Botany 57, 1677–1684. https://doi.org/10.1093/jxb/erl002

Krinsky, N. I. (1977). Singlet oxygen in biological systems.

Lea-Smith DJ, Bombelli P, Dennis JS, Scott SA, Smith AG, Howe CJ. (2014) Phycobilisome-deficient strains of *Synechocystis* sp. PCC 6803 have reduced size and require carbon-limiting conditions to exhibit enhanced productivity. Plant Physiology 165, 705-714. https://doi.org/ 10.1104/pp.114.237206.

Lee, H.Y., Hong, Y.N., Chow, W.S., (2001). Photoinactivation of photosystem II complexes and photoprotection by non-functional neighbors in *Capsicum annuum* L. leaves. Planta 212, 332–342. https://doi.org/10.1007/s004250000398

Lee, P. C., & Rodgers, M. A. J. (1983). Singlet molecular oxygen in micellar systems. 1. Distribution equilibria between hydrophobic and hydrophilic compartments. The Journal of Physical Chemistry 87, 4894-4898. https://doi.org/ 10.1021/j150642a027

Li, X., Hou, W., Lei, J., Chen, H., & Wang, Q. (2023). The unique light-harvesting system of the algal phycobilisome: structure, assembly components, and functions. International Journal of Molecular Sciences 24, 9733. https://doi.org/10.3390/ijms24119733

Li, X.-P., Björkman, O., Shih, C., Grossman, A. R., Rosenquist, M., Jansson, S., & Niyogi, K. K. (2000). A pigment-binding protein essential for regulation of photosynthetic light harvesting. Nature 403, 391–395. https://doi.org/10.1038/35000131

Martin, W., & Kowallik, K. (1999). Annotated english translation of mereschkowsky's 1905 paper "Über natur und ursprung der chromatophoren impflanzenreiche". European Journal of Phycology 34, 287–295. https://doi.org/10.1080/09670269910001736342

Matsubara, S., & Chow, W. S. (2004). Populations of photoinactivated photosystem II reaction centers characterized by chlorophyll *a* fluorescence lifetime in vivo. Proceedings of the National Academy of Sciences of the United States of America 101, 18234–18239. https://doi.org/10.1073/pnas.0403857102

Mattila, H., Khorobrykh, S., Hakala-Yatkin, M., Havurinne, V., Kuusisto, I., Antal, T., Tyystjärvi, T., & Tyystjärvi, E. (2020). Action spectrum of the redox state of the plastoquinone pool defines its function in plant acclimation. Plant Journal 104, 1088–1104. https://doi.org/10.1111/tpj.14983

Mattila, H., Khorobrykh, S., Havurinne, V., & Tyystjärvi, E. (2015). Reactive oxygen species: Reactions and detection from photosynthetic tissues. Journal of Photochemistry and Photobiology 152, 176–214. https://doi.org/10.1016/j.jphotobiol.2015.10.001

Mattila, H., Mishra, K. B., Kuusisto, I., Mishra, A., Novotná, K., Šebela, D., & Tyystjärvi, E. (2020). Effects of low temperature on photoinhibition and singlet oxygen production in four natural accessions of *Arabidopsis*. Planta 252, 19. https://doi.org/10.1007/s00425-020-03423-0

Mattila, H., Mishra, S., Tyystjärvi, T., & Tyystjärvi, E. (2023). Singlet oxygen production by photosystem II is caused by misses of the oxygen evolving complex. New Phytologist 237, 113–125. https://doi.org/10.1111/nph.18514

Meyer, B., Schlodder, E., Dekker, J. P., & Witt, H. T. (1989). O_2 evolution and Chl (P_{680}^+) nanosecond reduction kinetics in single flashes as a function of pH. Biochimica et Biophysica Acta – Bioenergetics 974, 36-43. https://doi.org/10.1016/S0005-2728(89)80163-X

Meyer, T. J., Huynh, M. H. V., & Thorp, H. H. (2007). The possible role of proton-coupled electron transfer (PCET) in water oxidation by photosystem II. Angewandte Chemie (International ed. in English) 46, 5284–5304. https://doi.org/10.1002/anie.200600917

Minagawa, J. (2011). State transitions-the molecular remodeling of photosynthetic supercomplexes that controls energy flow in the chloroplast. Biochimica et Biophysica Acta - Bioenergetics 1807, 897–905. https://doi.org/10.1016/j.bbabio.2010.11.005

Mishra, N. P., Francke, C., Van Gorkom, H. J., & Ghanotakis, D. F. (1994). Destructive role of singlet oxygen during aerobic illumination of the photosystem II core complex. Biochimica et Biophysica Acta – Bioenergetics 1186, 81-90. https://doi.org/10.1016/0005-2728(94)90138-4.

Miyao, M., Ikeuchi, M., Yamamoto, N., & Ono, T. (1995). Specific degradation of the D1 protein of photosystem II by treatment with hydrogen peroxide in darkness: implications for the mechanism of degradation of the D1 protein under illumination. Biochemistry 34, 10019–10026. https://doi.org/10.1021/bi00031a025

Mullineaux, C. W. (2008). Phycobilisome-reaction centre interaction in cyanobacteria. Photosynthesis Research 95, 175–182. https://doi.org/10.1007/s11120-007-9249-y

Mullineaux, C. W., & Allen, J. F. (1988). Fluorescence induction transients indicate dissociation of photosystem II from the phycobilisome during the state-2 transition in the cyanobacterium *Synechococcus* 6301. Biochimica et Biophysica Acta - Bioenergetics 934, 96–107. https://doi.org/10.1016/0005-2728(88)90124-7

Nath, K., Jajoo, A., Poudyal, R. S., Timilsina, R., Park, Y. S., Aro, E. M., Nam, H. G., & Lee, C. H. (2013). Towards a critical understanding of the photosystem II repair mechanism and its regulation during stress conditions. FEBS Letters 587, 3372–3381. https://doi.org/10.1016/j.febslet.2013.09.015

Nishiyama, Y., Allakhverdiev, S. I., Yamamoto, H., Hayashi, H., & Murata, N. (2004). Singlet oxygen inhibits the repair of photosystem II by suppressing the translation elongation of the D1 protein in *Synechocystis* sp. PCC 6803. Biochemistry 43, 11321–11330. https://doi.org/10.1021/bi036178q

Niyogi, K. K., & Truong, T. B. (2013). Evolution of flexible non-photochemical quenching mechanisms that regulate light harvesting in oxygenic photosynthesis. Current Opinion in Plant Biology 16, 307–314. https://doi.org/10.1016/j.pbi.2013.03.011

Novoderezhkin, V. I., Dekker, J. P., & Van Grondelley, R. (2007). Mixing of exciton and charge-transfer states in photosystem II reaction centers: Modeling of stark spectra with modified redfield theory. Biophysical Journal 93, 1293–1311. https://doi.org/10.1529/biophysj .106.096867

Ohnishi, N., Allakhverdiev, S. I., Takahashi, S., Higashi, S., Watanabe, M., Nishiyama, Y., & Murata, N. (2005). Two-step mechanism of photodamage to photosystem II: Step 1 occurs at the oxygen-evolving complex and step 2 occurs at the photochemical reaction center. Biochemistry 44, 8494–8499. https://doi.org/10.1021/bi047518q

Pham, L. V., Janna Olmos, J. D., Chernev, P., Kargul, J., & Messinger, J. (2019). Unequal misses during the flash-induced advancement of photosystem II: effects of the S state and acceptor side cycles. Photosynthesis Research 139, 93–106. https://doi.org/10.1007 /s11120-018-0574-0

Pinnola, A., & Bassi, R. (2018). Molecular mechanisms involved in plant photoprotection. Biochemical Society Transactions 46, 467–482. https://doi.org/10.1042/BST20170307

Pollari, M., Rantamäki, S., Huokko, T., Kårlund-Marttila, A., Virjamo, V., Tyystjärvi, E., & Tyystjärvi, T. (2011). Effects of deficiency and overdose of group 2 sigma factors in triple inactivation strains of *Synechocystis* sp. strain PCC 6803. Journal of Bacteriology. 193, 265–273. https://doi.org/10.1128/JB.01045-10

Pospíšil, P. (2016). Production of reactive oxygen species by photosystem II as a response to light and temperature stress. Frontiers in Plant Science. 7, 1950. https://doi.org/10.3389/ fpls.2016.01950

Quick, W. P., & Stitt, M. (1989). An examination of factors contributing to non-photochemical quenching of chlorophyll fluorescence in barley leaves. Biochimica et Biophysica Acta - Bioenergetics 977, 287-296. https://doi.org/10.1016/S0005-2728(89)80082-9.

Ranjbar Choubeh, R., Wientjes, E., Struik, P. C., Kirilovsky, D., & van Amerongen, H. (2018). State transitions in the cyanobacterium *Synechococcus elongatus* 7942 involve reversible

quenching of the photosystem II core. Biochimica et Biophysica Acta - Bioenergetics 1859, 1059–1066. https://doi.org/10.1016/j.bbabio.2018.06.008

Rappaport, F., Guergova-Kuras, M., Nixon, P. J., Diner, B. A., & Lavergne, J. (2002). Kinetics and pathways of charge recombination in photosystem II. Biochemistry 41, 8518–8527. https://doi.org/10.1021/bi025725p

Raszewski, G., Saenger, W., & Renger, T. (2005). Theory of optical spectra of photosystem II reaction centers: Location of the triplet state and the identity of the primary electron donor. Biophysical Journal 88, 986–998. https://doi.org/10.1529/biophysj.104.050294

Renger, G., & Renger, T. (2008). Photosystem II: The machinery of photosynthetic water splitting. Photosynthesis Research 98, 53–80. https://doi.org/10.1007/s11120-008-9345-7

Renger, G., & Wolff, C. (1976). The existence of a high photochemical turnover rate at the reaction centers of system II in Tris-washed chloroplasts. Biochimica et Biophysica Acta - Bioenergetics 423, 610–614. https://doi.org/10.1016/0005-2728(76)90214-0

Renger, T. (2009). Theory of excitation energy transfer: From structure to function. Photosynthesis Research 102, 471–485. https://doi.org/10.1007/s11120-009-9472-9

Rippka, E., Deruelles, J., & Waterbury, N. B. (1979). Generic assignments, strain histories and properties of pure cultures of cyanobacteria. Microbiology 111, 1-61. https://doi.org/10.1099/00221287-111-1-1

Romero, E., Van Stokkum, I. H. M., Novoderezhkin, V. I., Dekker, J. P., & Van Grondelle, R. (2010). Two different charge separation pathways in photosystem II. Biochemistry, 49, 4300–4307. https://doi.org/10.1021/bi1003926

Sacharz, J., Bryan, S. J., Yu, J., Burroughs, N. J., Spence, E. M., Nixon, P. J., & Mullineaux, C. W. (2015). Sub-cellular location of FtsH proteases in the cyanobacterium *Synechocystis* sp: PCC 6803 suggests localised PSII repair zones in the thylakoid membranes. Molecular Microbiology 96, 448–462. https://doi.org/10.1111/mmi.12940

Santabarbara, S., Neverov, K. V., Garlaschi, F. M., Zucchelli, G., & Jennings, R. C. (2001). Involvement of uncoupled antenna chlorophylls in photoinhibition in thylakoids. FEBS Letters 491, 109–113. https://doi.org/10.1016/S0014-5793(01)02174-3

Sarvikas, P., Hakala, M., Pätsikkä, E., Tyystjärvi, T., & Tyystjärvi, E. (2006). Action spectrum of photoinhibition in leaves of wild type and npq1-2 and npq4-1 mutants of *Arabidopsis thaliana*. Plant & Cell Physiology 47, 391–400. https://doi.org/10.1093/pcp/pcj006

Sarvikas, P., Tyystjärvi, T., & Tyystjärvi, E. (2010). Kinetics of prolonged photoinhibition revisited: Photoinhibited photosystem II centres do not protect the active ones against loss of oxygen evolution. Photosynthesis Research 103, 7–17. https://doi.org/10.1007/s11120-009-9496-1

Schatz, G. H., Brock, H., & Holzwarth, A. R. (1987). Picosecond kinetics of fluorescence and absorbance changes in photosystem II particles excited at low photon density. In Proceedings of the National Academy of Sciences of the United States of America 84, 8414–8418. https://doi.org/10.1073/pnas.84.23.8414

Schweitzer, C., & Schmidt, R. (2003). Physical mechanisms of generation and deactivation of singlet oxygen. Chemical Reviews 103, 1685–1757. https://doi.org/10.1021/cr010371d

Service, R. J., Hillier, W., & Debus, R. J. (2010). Evidence from FTIR difference spectroscopy of an extensive network of hydrogen bonds near the oxygen-evolving Mn_4Ca cluster of photosystem II involving D1-Glu65, D2-Glu312, and D1-Glu329. Biochemistry 49, 6655–6669. https://doi.org/10.1021/bi100730d

Sessions, A. L., Doughty, D. M., Welander, P. V., Summons, R. E., & Newman, D. K. (2009). The continuing puzzle of the Great Oxidation Event. Current Biology 19, R567–R574. https://doi.org/10.1016/j.cub.2009.05.054

Shapiguzov, A., Ingelsson, B., Samol, I., Andres, C., Kessler, F., Rochaix, J. D., Vener, A. V., & Goldschmidt-Clermont, M. (2010). The PPH1 phosphatase is specifically involved in LHCII dephosphorylation and state transitions in Arabidopsis. Proceedings of the National Academy of Sciences of the United States of America, 107, 4782–4787. https://doi.org/10.1073/ pnas.0913810107

Sipka, G., Magyar, M., Mezzetti, A., Akhtar, P., Zhu, Q., Xiao, Y., Han, G., Santabarbara, S., Shen, J. R., Lambrev, P. H., & Garab, G. (2021). Light-adapted charge-separated state of photosystem II: Structural and functional dynamics of the closed reaction center. Plant Cell 33, 1286–1302. https://doi.org/10.1093/plcell/koab008

Sonoike, K. (2011). Photoinhibition of photosystem I. Physiologia Plantarum, 142, 56–64. https://doi.org/10.1111/j.1399-3054.2010.01437.x

Sopory, S. K., Greenbergb, B. M., Mehtaac, R. A., Edelmanab, M., & Mattooa, A. K. (1990). Free radical scavengers inhibit light-dependent degradation of the 32 kDa photosystem II reaction center protein. eitschrift für Naturforschung C 45, 412-417. https://doi.org/10.1515/znc-1990-0517

Suga, M., Akita, F., Hirata, K., Ueno, G., Murakami, H., Nakajima, Y., Shimizu, T., Yamashita, K., Yamamoto, M., Ago, H., & Shen, J. R. (2015). Native structure of photosystem II at 1.95Å resolution viewed by femtosecond X-ray pulses. Nature 517, 99–103. https://doi.org/10.1038/nature13991

Sun, Z. L., Lee, H. Y., Matsubara, S., Hope, A. B., Pogson, B. J., Hong, Y. N., & Chow, W. S. (2006). Photoprotection of residual functional photosystem II units that survive illumination in the absence of repair, and their critical role in subsequent recovery. Physiologia Plantarum 128, 415–424. https://doi.org/10.1111/j.1399-3054.2006.00754.x

Takahashi, Y., Hansson, O., Mathis, P., & Satoh, K. (1987). Primary radical pair in the photosystem II reaction centre. Biochimica et Biophysica Acta – Bioenergetics 893, 49-59. https://doi.org/10.1016/0005-2728(87)90147-2.

Tian, L., Van Stokkum, I. H. M., Koehorst, R. B. M., Jongerius, A., Kirilovsky, D., & Van Amerongen, H. (2011). Site, rate, and mechanism of photoprotective quenching in cyanobacteria. Journal of the American Chemical Society 133, 18304–18311. https://doi.org/ 10.1021/ja206414m

Tikkanen, M., Grieco, M., & Aro, E. M. (2011). Novel insights into plant light-harvesting complex II phosphorylation and “state transitions”. Trends in Plant Science 16, 126–131. https://doi.org/10.1016/j.tplants.2010.11.006

Tikkanen, M., Mekala, N. R., & Aro, E. M. (2014). Photosystem II photoinhibition-repair cycle protects Photosystem I from irreversible damage. Biochimica et Biophysica Acta - Bioenergetics 1837, 210–215. https://doi.org/10.1016/j.bbabio.2013.10.001

Tiwari, A., Mamedov, F., Grieco, M., Suorsa M., Jajoo, A., Styring, S., Tikkanen, M., Aro, E.–M. (2016) Photodamage of iron–sulphur clusters in photosystem I induces non-photochemical energy dissipation. Nature Plants 2, 16035. https://doi.org/10.1038/nplants.2016.35

Tsonev, T. D., & Hikosaka, K. (2003). Contribution of photosynthetic electron transport, heat dissipation, and recovery of photoinactivated photosystem II to photoprotection at different temperatures in chenopodium album leaves. Plant & Cell Physiology 44, 828–835. https://doi.org/10.1093/pcp/pcg107

Tyystjärvi, E. (2013). Photoinhibition of Photosystem II. International Review of Cell and Molecular Biology 300, 243–303. https://doi.org/10.1016/B978-0-12-405210-9.00007-2

Tyystjärvi, E., & Aro, E.-M. (1996). The rate constant of photoinhibition, measured in lincomycin-treated leaves, is directly proportional to light intensity. Proceedings of the National Academy of Sciences of the United States of America, 93, 2213–2218. https://doi.org/10.1073/ pnas.93.5.2213

Tyystjärvi E, Kettunen R, Aro E-M. (1994). The rate constant of photoinhibition *in vitro* is independent of the antenna size of photosystem II but depends on temperature. Biochimica et Biophysica Acta – Bioenergetics 1186, 177–185. https://doi.org/10.1016/0005-2728(94)90177-5

Ueno, M., Sae-Tang, P., Kusama, Y., Hihara, Y., Matsuda, M., Hasunuma, T., & Nishiyama, Y. (2016). Moderate heat stress stimulates repair of photosystem II during photoinhibition in *Synechocystis* sp. PCC 6803. Plant & Cell Physiology 57, 2417–2426. https://doi.org/10.1093/pcp/pcw153

Umena, Y., Kawakami, K., Shen, J. R., & Kamiya, N. (2011). Crystal structure of oxygen-evolving photosystem II at a resolution of 1.9Å. Nature 473, 55–60. https://doi.org/10.1038/nature09913

van Amerongen, H., & Chmeliov, J. (2020). Instantaneous switching between different modes of non-photochemical quenching in plants. Consequences for increasing biomass production. Biochimica et Biophysica Acta - Bioenergetics 1861, 148119. https://doi.org/10.1016/ j.bbabio.2019.148119

Vasil’ev, S., Bergmann, A., Redlin, H., Eichler, H.-J., & Renger, G. (1996). On the role of exchangeable hydrogen bonds for the kinetics of $P_{680}^{+}\cdot$ $Q_A^{-}\cdot$ formation and $P_{680}^{+}\cdot$ $Pheo^{-}\cdot$ recombination in photosystem II. Biochimica et Biophysica Acta – Bioenergetics 1276, 35-44, https://doi.org/10.1016/0005-2728(96)00027-8

Vass, I. (2011). Role of charge recombination processes in photodamage and photoprotection of the photosystem II complex. Physiologia Plantarum 142, 6–16. https://doi.org /10.1111/j.1399-3054.2011.01454.x

Vass, I. (2012). Molecular mechanisms of photodamage in the Photosystem II complex. In Biochimica et Biophysica Acta - Bioenergetics 1817, 209–217. https://doi.org/10.1016/ j.bbabio.2011.04.014

Vass, I., & Cser, K. (2009). Janus-faced charge recombinations in photosystem II photoinhibition. Trends in Plant Science 14, 200–205. https://doi.org/10.1016 /j.tplants.2009.01.009

Vass, I., & Styring, S. (1993). Characterization of chlorophyll triplet promoting states in photosystem II sequentially induced during photoinhibition. Biochemistry 32, 3334–3341. https://doi.org/10.1021/bi00064a016. https://pubs.acs.org/sharingguidelines

Vass, I., Styring, S., Hundal, T., Koivuniemi, A., Aro, E.-M., & Andersson, B. (1992). Reversible and irreversible intermediates during photoinhibition of photosystem II: Stable reduced Q_A species promote chlorophyll triplet formation. Proceedings of the National Academy of Sciences of the United States of America 89, 1408–1412. https://doi.org/10.1073/ pnas.89.4.1408 Vol. 89)

Vener, A. V, Van Kan, P. J. M., Rich, P. R., Ohad, I., & Andersson, B. (1997). Plastoquinol at the quinol oxidation site of reduced cytochrome bf mediates signal transduction between light and protein phosphorylation: Thylakoid protein kinase deactivation by a single-turnover flash. Proceedings of the National Academy of Sciences of the United States of America 94, 1585–1590. https://doi.org/10.1073/pnas.94.4.1585

Wei, X., Su, X., Cao, P., Liu, X., Chang, W., Li, M., Zhang, X., & Liu, Z. (2016). Structure of spinach photosystem II-LHCII supercomplex at 3.2 Å resolution. Nature 534, 69–74. https://doi.org/10.1038/nature18020

Wilson, A., Punginelli, C., Gall, A., Bonetti, C., Alexandre, M., Routaboul, J.-M., Kerfeld, C. A., Van Grondelle, R., Robert, B., Kennis, J. T. M., & Kirilovsky, D. (2008). A photoactive carotenoid protein acting as light intensity sensor. Proceedings of the National Academy of Sciences of the United States of America 105, 12075–12080. https://doi.org/10.1073/pnas.0804636105

Wraight, C. A., & Crofts, A. R. (1970). Energy-dependent quenching of chlorophyll *a* fluorescence in isolated chloroplasts. European Journal of Biochemistry 17, 319–327. https://doi.org/10.1111/j.1432-1033.1970.tb01169.x